

Denoising Diffused Embeddings: a Generative Approach for Hypergraphs

Shihao Wu, Junyi Yang, Gongjun Xu, and Ji Zhu
Department of Statistics, University of Michigan

Abstract

Hypergraph data, which capture multi-way interactions among entities, are becoming increasingly prevalent in the big data era. Generating new hyperlinks from an observed, usually high-dimensional hypergraph is an important yet challenging task with diverse applications, such as electronic health record analysis and biological research. This task is fraught with several challenges. The discrete nature of hyperlinks renders many existing generative models inapplicable. Additionally, powerful machine learning-based generative models often operate as black boxes, providing limited interpretability. Key structural characteristics of hypergraphs, including node degree heterogeneity and hyperlink sparsity, further complicate the modeling process and must be carefully addressed. To tackle these challenges, we propose Denoising Diffused Embeddings (DDE), a general generative model architecture for hypergraphs. DDE exploits potential low-rank structures in high-dimensional hypergraphs and adopts the state-of-the-art diffusion model framework. Theoretically, we show that when true embeddings are accessible, DDE exactly reduces the task of generating new high-dimensional hyperlinks to generating new low-dimensional embeddings. Moreover, we analyze the implications of using estimated embeddings in DDE, revealing how hypergraph properties—such as dimensionality, node degree heterogeneity, and hyperlink sparsity—impact its generative performance. Simulation studies demonstrate the superiority of DDE over existing methods, in terms of both computational efficiency and generative accuracy. Furthermore, an application to a symptom co-occurrence hypergraph derived from electronic medical records uncovers interesting findings and highlights the advantages of DDE.

Keywords: hypergraphs, generative models, latent embeddings, diffusion models.

1 Introduction

Hypergraph data, which capture multi-way interactions among entities, are increasingly prevalent in the big data era. For example, the Medical Information Mart for Intensive Care dataset (MIMIC-III; [Johnson et al. 2016](#)) includes clinical records from 49,785 hospital admissions involving 38,597 unique adult patients. These records document the co-occurrence of clinical symptoms and procedures within patient profiles, capturing the underlying relationships among medical symptoms and procedures. Similarly, in protein interaction datasets ([Rhodes et al. 2005](#), [Nepusz et al. 2012](#)), groups of proteins function together in metabolic reactions, while in gene interaction datasets ([Rinaldo et al. 2005](#), [Shojaie & Michailidis 2009](#)), groups of genes associate with each other to potentially form protein complexes. These interactions, which can be represented by hypergraphs, provide valuable insights into the functional roles of genes and proteins in biological processes.

A hypergraph can be denoted by $\mathcal{H}(\mathcal{V}_n, \mathcal{E}_m)$, which consists of the node set $\mathcal{V}_n = \{v_1, \dots, v_n\}$ and a collection of hyperlinks/hyperedges $\mathcal{E}_m = \{e_1, \dots, e_m\}$. For simplicity, we denote $\mathcal{V}_n = [n] = \{1, \dots, n\}$. Each hyperlink is a subset of $[n]$, representing the nodes on that hyperlink. For example, if $e_1 = \{1, 2, 3\}$, then nodes 1, 2 and 3 form hyperlink 1. Figure 1 illustrates an example of an observed hypergraph with 9 nodes and 4 *observed* hyperlinks. Hyperlinks have an *order*, defined as the number of nodes they contain. In Fig-

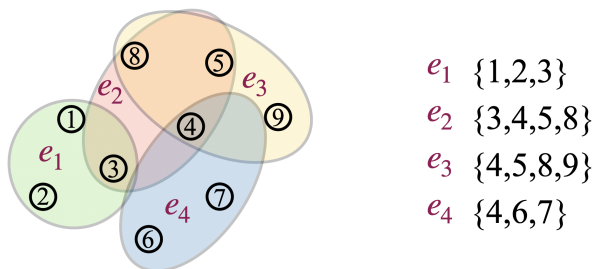


Figure 1: Example of an observed hypergraph $\mathcal{H}([9], \{e_1, e_2, e_3, e_4\})$. The hyperlinks observed from the hypergraph in the left figure are shown as a set of sets on the right.

Figure 1, the four hyperlinks have orders of 3, 4, 4, and 3, respectively. Moreover, the nodes in a hypergraph typically exhibit *heterogeneous degrees*, reflecting their varying “popularity”. For example, in Figure 1, node 4 appears 3 times among the four observed hyperlinks, indicating a higher degree than node 2, which appears only once. Besides node degree heterogeneity, another characteristic of real-world hypergraphs is the sparsity of hyperlinks: the orders of the hyperlinks are usually much smaller in comparison to the total number of nodes. For instance, in the MIMIC-III dataset, a symptom co-occurrence hypergraph can be constructed where medical symptoms are nodes, and each patient profile forms a hyperlink, with nodes representing the symptoms exhibited by the patient. This hypergraph contains 6,985 nodes and 49,785 hyperlinks, with median and mean hyperlink orders of 9 and 12.6, respectively, highlighting the sparsity of the hyperlinks relative to the total number of nodes. Moreover, the node degrees in this hypergraph are highly heterogeneous, as indicated by the 25th and 75th percentiles of node frequencies, which are 2 and 27, respectively.

In this work, we study generative models for hypergraphs, which aim to generate new hyperlinks based on an observed hypergraph. Synthetic hyperlink generation has significant applications in modern data analysis. For instance, in electronic health record data, symptom co-occurrences in patient profiles can be represented as hyperlinks. Since each medical center typically has a limited number of patient profiles, deeper and more accurate analyses often require data sharing across centers. However, directly sharing these hyperlinks raises privacy concerns. Generating synthetic hyperlinks that closely match the distribution to real ones while remaining distinct offers a practical solution. These synthetic hyperlinks enable data pooling across medical centers, facilitating richer analyses while preserving patient privacy. Other examples of applications include generating new combinations of protein or gene subgroups that may function together, creating product bundles for online shoppers, and designing new recipes by combining various ingredients.

The generated hyperlinks should have several desirable properties. In particular, they must avoid being exact replicas of existing hyperlinks, while they should follow a distribution similar to those in the observed hypergraph. More specifically, the new hypergraph formed by these generated hyperlinks should preserve key characteristics of the observed hypergraph, such as node degree heterogeneity and hyperlink sparsity. In the following section, we introduce our proposed approach, termed Denoising Diffused Embeddings (DDE), designed to address these requirements.

1.1 Denoising Diffused Embeddings (DDE)

Given an observed hypergraph $\mathcal{H}([n], \mathcal{E}_m)$, DDE outputs a synthetic hypergraph $\tilde{\mathcal{H}}([n], \tilde{\mathcal{E}}_{\tilde{m}})$, where $\tilde{\mathcal{E}}_{\tilde{m}} = \{\tilde{e}_1, \dots, \tilde{e}_{\tilde{m}}\}$ represents the set of newly generated hyperlinks and \tilde{m} denotes the number of these hyperlinks. Assume that each node i is associated with a latent embedding \mathbf{z}_i and a node degree parameter $\alpha_i \in \mathbb{R}$. Furthermore, a hyperlink e is generated based on its associated hyperlink embedding \mathbf{x} , with its distribution determined by a conditional likelihood model $\mathbb{P}_{\mathcal{H}([n], \{E\}) | \mathbf{x}, \mathcal{Z}_n, \boldsymbol{\alpha}_n}$, where E denotes a random hyperlink, $\mathcal{Z}_n = \{\mathbf{z}_1, \dots, \mathbf{z}_n\}$, and $\boldsymbol{\alpha}_n = (\alpha_1, \dots, \alpha_n)^\top$. DDE allows the embeddings to reside in general latent spaces, including Euclidean and hyperbolic spaces (see Section 2 for details). Let $\mathcal{X}_m = \{\mathbf{x}_1, \dots, \mathbf{x}_m\}$ collect the hyperlink embeddings corresponding to the observed hypergraph $\mathcal{H}([n], \mathcal{E}_m)$. Consider a hypothetical *random* hypergraph $\mathcal{H}_{m,n} := \mathcal{H}([n], \{E_1, \dots, E_m\})$, from which $\mathcal{H}([n], \mathcal{E}_m)$ is a single realization. Let $\mathbb{P}_{\mathcal{H}_{m,n} | \mathcal{X}_m, \mathcal{Z}_n, \boldsymbol{\alpha}_n}$ denote its distribution given the latent embeddings and node degree parameters. We impose the following condition.

Condition 1.1. $\mathbb{P}_{\mathcal{H}_{m,n} | \mathcal{X}_m, \mathcal{Z}_n, \boldsymbol{\alpha}_n}$ satisfies that $\mathbb{P}_{\mathcal{H}_{m,n} | \mathcal{X}_m, \mathcal{Z}_n, \boldsymbol{\alpha}_n} = \prod_{j=1}^m \mathbb{P}_{\mathcal{H}([n], \{E_j\}) | \mathbf{x}_j, \mathcal{Z}_n, \boldsymbol{\alpha}_n}$.

Condition 1.1 ensures the *conditional independence* of hyperlinks given all the embeddings and degree parameters. This conditional independence implies that each round of co-occurrence among the nodes can be fully characterized by the embeddings. Simi-

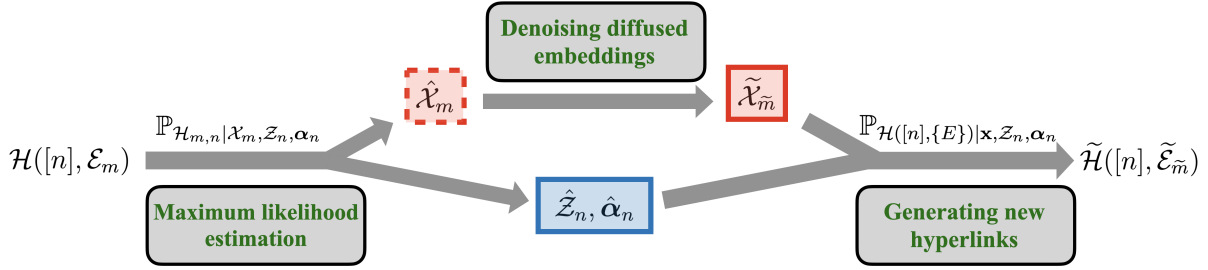


Figure 2: Denoising Diffused Embeddings.

lar assumptions have been widely adopted in hypergraph analysis, e.g., Ke et al. (2019), Yuan & Qu (2023), and Zhen & Wang (2023). For a pre-determined conditional model $\mathbb{P}_{\mathcal{H}_{m,n}|\mathcal{X}_m, \mathcal{Z}_n, \alpha_n} = \prod_{j=1}^m \mathbb{P}_{\mathcal{H}([n], \{E_j\})|\mathbf{x}_j, \mathcal{Z}_n, \alpha_n}$, we summarize DDE in Figure 2. Specifically, DDE consists of three steps: 1) Parameter estimation. Using maximum likelihood estimation based on $\mathbb{P}_{\mathcal{H}_{m,n}|\mathbf{x}, \mathcal{Z}_n, \alpha_n}$ and the observed hypergraph $\mathcal{H}([n], \mathcal{E}_m)$, we obtain estimators for the hyperlink embeddings, node embeddings, and degree parameters, denoted as $\hat{\mathcal{X}}_m = \{\hat{\mathbf{x}}_1, \dots, \hat{\mathbf{x}}_m\}$, $\hat{\mathcal{Z}}_n = \{\hat{\mathbf{z}}_1, \dots, \hat{\mathbf{z}}_n\}$, and $\hat{\alpha}_n = (\hat{\alpha}_1, \dots, \hat{\alpha}_n)^\top$, respectively. 2) Hyperlink embedding generation. A new set of hyperlink embeddings, $\tilde{\mathcal{X}}_m = \{\tilde{\mathbf{x}}_1, \dots, \tilde{\mathbf{x}}_m\}$, is generated using diffusion models (Sohl-Dickstein et al. 2015, Song et al. 2020, Ho et al. 2020), a class of generative models trained on $\hat{\mathcal{X}}_m$. 3) Hypergraph generation. Using $\tilde{\mathcal{X}}_m$, $\hat{\mathcal{Z}}_n$, and $\hat{\alpha}_n$, a new hypergraph is generated based on the conditional model $\prod_{j=1}^{\tilde{m}} \mathbb{P}_{\mathcal{H}([n], \{\tilde{E}_j\})|\tilde{\mathbf{x}}_j, \hat{\mathcal{Z}}_n, \hat{\alpha}_n}$. A detailed description of DDE is provided in Section 2.

1.2 Related work

With the rise of hypergraph data in the big data era, the modeling and analysis of hypergraph structures have garnered significant attention. Ke et al. (2019) highlighted that previous approaches projecting hypergraphs onto weighted graphs (Ghoshdastidar & Dukkipati 2015, Kumar et al. 2018, Lee et al. 2020) often lead to information loss, yielding suboptimal community detection results. With regard to direct modeling of hypergraphs, Ke et al.

(2019) generalized the hypergraph planted partition model in Ghoshdastidar & Dukkipati (2017) and proposed a tensor-based algorithm for community detection. Yuan & Qu (2023) and Zhen & Wang (2023) modeled hypergraphs in latent spaces, and Yuan et al. (2022) studied statistical inference for hypergraph objectives. Despite this progress, these methods heavily rely on uniform restrictions of hyperlink orders and cannot handle the multiplicity of hyperlinks, i.e., multiple occurrences of the same hyperlink within a hypergraph. To overcome these limitations, Wu et al. (2024) proposed a latent embedding framework that supports varying hyperlink orders and repeated hyperlinks. This approach allows for individual embeddings for both nodes and hyperlinks in the hypergraph, aligning well with the framework presented in this paper. While the modeling of observed hypergraphs has been extensively explored, the generation of new hypergraphs from an observed one, i.e., developing generative models for hypergraphs, remains underexplored. In light of the growing demand for generating hyperlinks with high fidelity, this work aims to address this critical gap.

Generative models are designed to produce data that mimics the features and structures of real-world observed data. Among these, diffusion models (Sohl-Dickstein et al. 2015, Song et al. 2020, Ho et al. 2020) have recently revolutionized applications such as image and audio generation, outperforming previous state-of-the-art methods like generative adversarial networks (Creswell et al. 2018, Goodfellow et al. 2020) and variational autoencoders (Kingma 2013, Kingma et al. 2019). For an overview of recent progress on diffusion models, see Chen et al. (2024). Despite numerous methodological innovations, most diffusion models operate in continuous spaces. However, the discrete nature of hyperlinks requires generative models tailored to discrete spaces. Existing graph generative models (You et al. 2018, Chen, He, Han & Liu 2023) focus on generating new discrete adjacency matrices, which are unsuitable for hyperlink generation because hyperlinks are discrete sets that cannot be represented by adjacency matrices. Efforts to extend diffusion

models to general discrete data include [Austin et al. \(2021\)](#) and [Lou et al. \(2024\)](#), but these approaches are computationally intensive. They work directly with high-dimensional discrete variables and fail to account for the unique properties of hypergraphs, such as their low-rank structures ([Thibeault et al. 2024](#)). Consequently, these methods may suffer from slow sampling convergence and suboptimal estimation performance.

In contrast, DDE first projects the high-dimensional hyperlinks onto a continuous and potentially low-dimensional space. It then leverages the strengths of diffusion models in continuous spaces, enabling a fast and accurate generation process. The idea of incorporating low-dimensional structures in latent spaces for diffusion models has also been explored in recent studies. With different training strategies, [Vahdat et al. \(2021\)](#) and [Rombach et al. \(2022\)](#) combined diffusion models with autoencoder architectures to operate in the latent semantic spaces for image generation. However, these approaches do not consider the unique characteristics of hypergraphs and lack interpretability, as the newly generated data is produced as purely black-box outputs. In contrast, DDE incorporates a likelihood modeling component that preserves key properties of hypergraphs, such as node degree heterogeneity and hyperlink sparsity, ensuring both interpretability and fidelity in the generated data. When data resides on an unknown low-dimensional linear subspace, [Chen, Huang, Zhao & Wang \(2023\)](#) adapted the score network architecture to align with this structure and theoretically demonstrated that such modification allows diffusion models to circumvent the curse of ambient dimensionality. In [Section 3](#), we show that DDE provides a general solution for overcoming the curse of ambient dimensionality in high-dimensional hypergraphs. Additionally, we present a theoretical comparison between the approach proposed by [Chen, Huang, Zhao & Wang \(2023\)](#) and DDE in [Section 3.1](#).

1.3 Contribution

The contribution of this work can be summarized into two main aspects. Methodologically, we propose a general generative model architecture, DDE, specifically designed for hypergraphs. DDE leverages the unique properties of hypergraphs through likelihood modeling, while incorporating state-of-the-art diffusion models for flexible and efficient sampling of new latent hyperlink embeddings. This combination results in a faster and more accurate sampling process compared to existing methods. We demonstrate the advantages of DDE over competing approaches using both simulated and real-world data.

Theoretically, we investigate the generative performance of DDE under both ideal and practical conditions. In scenarios of perfect embedding estimation, where the node and hyperlink embeddings generating the observed hypergraph are accurately recovered, DDE fully circumvents the curse of data ambient dimensionality. Specifically, while a subset of $[n]$ can be encoded as a vector in $\{0,1\}^n$, we show that DDE reduces the task of generating n -dimensional discrete vectors to generating K -dimensional embeddings, where K , the latent space dimension, can be substantially smaller than n . Furthermore, we study how the embedding estimation procedure impacts the generative performance, highlighting the roles of dimensionality, node degree heterogeneity, and hyperlink sparsity of the hypergraph. These technical results not only advance theoretical understanding but also provide practical guidance for applying DDE effectively in hypergraph generative modeling, clarifying the conditions under which it performs optimally.

1.4 Organization of the paper and notations

The remainder of this article is organized as follows. Section 2 introduces the DDE framework. Section 3 analyzes the generative performance of DDE. Section 4 provides numerically comparisons of DDE with competing approaches. Section 5 applies DDE to the

MIMIC-III dataset, generating new patient profiles and uncovering interesting discoveries. Finally, Section 6 concludes the paper with a discussion. The supplementary material includes proofs of the main results, technical lemmas with their proofs, and additional numerical results.

For any $a, b \in \mathbb{R}$, we denote their maximum and minimum by $a \vee b = \max(a, b)$ and $a \wedge b = \min(a, b)$, respectively. Given any two sequences $(a_{m,n}), (b_{m,n})$ valued in \mathbb{R} , we say $a_{m,n} \lesssim b_{m,n}$ (or $a_{m,n} = O(b_{m,n}), b_{m,n} \gtrsim a_{m,n}$) if there exists a universal constant $C > 0$ such that $|a_{m,n}| \leq C|b_{m,n}|$ as $m, n \rightarrow \infty$. We say $a_{m,n} \asymp b_{m,n}$ if $a_{m,n} \lesssim b_{m,n}$ and $a_{m,n} \gtrsim b_{m,n}$. We write $a_{m,n} \ll b_{m,n}$ (or $a_{m,n} = o(b_{m,n})$) if $\lim_{m,n \rightarrow \infty} a_{m,n}/b_{m,n} = 0$ and $a_{m,n} \gg b_{m,n}$ (or $a_{m,n} = \Omega(b_{m,n})$) if $\lim_{m,n \rightarrow \infty} a_{m,n}/b_{m,n} = \infty$. We use $O_p(\cdot), \Omega_p(\cdot)$, and $o_p(\cdot)$ as the stochastic versions of $O(\cdot), \Omega(\cdot)$, and $o(\cdot)$ for convergence in probability. For any positive integer a , we use $[a]$ to denote the set $\{1, 2, \dots, a\}$. For any column vector \mathbf{a} and matrix \mathbf{A} , we use \mathbf{a}^\top and \mathbf{A}^\top to denote their transposes, respectively. For an event \mathfrak{E} , the indicator function $\mathbf{1}_{\mathfrak{E}} = 1$ if \mathfrak{E} occurs and 0 otherwise. For a vector $\mathbf{a} = (a_1, \dots, a_n)^\top$, we use $\|\mathbf{a}\|_2$ to denote the standard Euclidean norm and $\|\mathbf{a}\|_\infty = \max_i |a_i|$ to denote the infinity/maximum/supreme norm. For a matrix $\mathbf{A} = (a_{ji})_{m \times n}$, we use $\|\mathbf{A}\|_2$ and $\|\mathbf{A}\|_{\max} = \max_{j \in [m], i \in [n]} |a_{ji}|$ to denote its spectrum and maximum/supreme norms, respectively. For a square matrix \mathbf{A} , we use $\lambda_{\max}(\mathbf{A})$ and $\lambda_{\min}(\mathbf{A})$ to denote its maximal and minimal eigenvalues, respectively. For probability measures \mathbb{P}_1 and \mathbb{P}_2 defined on a measurable space (Ω, \mathcal{F}) , we denote their total variation distance as $d_{\text{TV}}(\mathbb{P}_1, \mathbb{P}_2) = \sup_{A \in \mathcal{F}} |\mathbb{P}_1(A) - \mathbb{P}_2(A)|$ and KL (Kullback-Leibler) divergence as $d_{\text{KL}}(\mathbb{P}_1 \parallel \mathbb{P}_2) = \int_{a \in \Omega} \log \{ \mathbb{P}_1(da) / \mathbb{P}_2(da) \} \mathbb{P}_1(da)$, respectively, where $\mathbb{P}_1(da) / \mathbb{P}_2(da)$ is the Radon-Nikodym derivative of \mathbb{P}_1 with respect to \mathbb{P}_2 .

2 Methodology

In this section, we provide a detailed introduction to DDE. Algorithm 1 illustrates the process by which DDE generates \tilde{m} new hyperlinks from an observed hypergraph $\mathcal{H}([n], \mathcal{E}_m)$. There are two modeling components in Algorithm 1. The first is the conditional likelihood hypergraph model, which builds the connection between the hypergraph and a latent space. The second is a diffusion model architecture that is to be trained on the latent space and to sample new hyperlinks from. We next discuss these two modeling components and their implementation in Algorithm 1.

Algorithm 1: Denoising Diffused Embeddings (DDE)

Input: Hypergraph $\mathcal{H}([n], \mathcal{E}_m)$; Number of new hyperlinks \tilde{m} ; Conditional hypergraph model $\mathbb{P}_{\mathcal{H}_{m,n}|\mathcal{X}_m, \mathcal{Z}_n, \alpha_n} = \prod_{j=1}^m \mathbb{P}_{\mathcal{H}([n], E_j)|\mathbf{x}_j, \mathcal{Z}_n, \alpha_n}$; Diffusion model architecture \mathcal{M} .

- 1 *Maximum likelihood estimation:* Based on the conditional hypergraph model $\mathbb{P}_{\mathcal{H}_{m,n}|\mathcal{X}_m, \mathcal{Z}_n, \alpha_n}$ and the observed hypergraph $\mathcal{H}([n], \mathcal{E}_m)$, obtain estimated node embeddings $\hat{\mathcal{Z}}_n = \{\hat{\mathbf{z}}_1, \dots, \hat{\mathbf{z}}_n\}$, estimated node degrees $\hat{\alpha}_n = (\hat{\alpha}_1, \dots, \hat{\alpha}_n)^\top$ and estimated embeddings for the observed hyperlinks $\hat{\mathcal{X}}_m = \{\hat{\mathbf{x}}_1, \dots, \hat{\mathbf{x}}_m\}$.
- 2 *Denoising diffused embeddings:* Train the diffusion model architecture \mathcal{M} on $\hat{\mathcal{X}}_m$ to get a sampler $\hat{\mathcal{F}}$ and sample \tilde{m} hyperlink embeddings $\tilde{\mathcal{X}}_{\tilde{m}} = \{\tilde{\mathbf{x}}_1, \dots, \tilde{\mathbf{x}}_{\tilde{m}}\}$ from $\hat{\mathcal{F}}$.
- 3 *Generating hyperlinks from the embeddings:* Generate a new hypergraph $\tilde{\mathcal{H}}([n], \tilde{\mathcal{E}}_{\tilde{m}}) = \tilde{\mathcal{H}}([n], (\tilde{e}_1, \dots, \tilde{e}_{\tilde{m}}))$ based on $\mathbb{P}_{\mathcal{H}([n], E)|\mathbf{x}, \mathcal{Z}_n, \alpha_n}$ where \mathcal{Z}_n and α_n are replaced by $\hat{\mathcal{Z}}_n$ and $\hat{\alpha}_n$, and each \mathbf{x} is plugged in by $\tilde{\mathbf{x}}_j$ for $j \in [\tilde{m}]$.

Output: $\tilde{\mathcal{H}}([n], \tilde{\mathcal{E}}_{\tilde{m}})$.

For the conditional likelihood hypergraph model, consider the hypothetical hypergraph $\mathcal{H}_{m,n} = \mathcal{H}([n], \{E_1, \dots, E_m\})$, with each E_j being a random subset of $[n]$. Let $\mathcal{P}(\mathcal{A})$ denote the power set of \mathcal{A} : $\mathcal{P}(\mathcal{A}) = \{A : A \subset \mathcal{A}\}$. Then $\mathcal{P}([n])$ collects all the possible hyperlinks

formed over n nodes. The observed hypergraph $\mathcal{H}([n], \{e_1, \dots, e_m\})$ is one realization of $\mathcal{H}([n], \{E_1, \dots, E_m\})$ valued on $\{\mathcal{P}([n])\}^m$. The conditional hypergraph model then specifies

$$\begin{aligned} & \mathbb{P}_{\mathcal{H}_{m,n}|\mathcal{X}_m, \mathcal{Z}_n, \alpha_n} \{ \mathcal{H}([n], \{E_1, \dots, E_m\}) = \mathcal{H}([n], \{e_1, \dots, e_m\}) \} \\ &= \prod_{j=1}^m \mathbb{P}_{\mathcal{H}([n], \{E_j\})|\mathbf{x}_j, \mathcal{Z}_n, \alpha_n} (E_j = e_j), \quad \text{for any } e_1, \dots, e_m \in \mathcal{P}([n]), \end{aligned} \tag{2.1}$$

through the independent hyperlink generating model $\mathbb{P}_{\mathcal{H}([n], \{E\})|\mathbf{x}, \mathcal{Z}_n, \alpha_n}$. The multiplicity form comes from the conditional independence assumption in Condition 1.1. Below are three examples of models under this framework.

Example 2.1 (Linear generation in Euclidean spaces (Wu et al. 2024)). Consider \mathbf{x} valued in \mathbb{R}^K and $\mathcal{Z}_n \subset \mathbb{R}^K$, where K is the latent Euclidean space dimension. Let $\sigma(a) := 1/(1 + \exp(-a))$ for $a \in \mathbb{R}$ and $p_i(\mathbf{x}) = \sigma(\mathbf{x}^\top \mathbf{z}_i + \alpha_i)$. We model the conditional probability as $\mathbb{P}_{\mathcal{H}([n], \{E\})|\mathbf{x}, \mathcal{Z}_n, \alpha_n} (E = e) = \prod_{i \in e} p_i(\mathbf{x}) \prod_{i \in [n] \setminus e} \{1 - p_i(\mathbf{x})\}$ for $e \in \mathcal{P}([n])$ in (2.1). As discussed in Wu et al. (2024), this linear embedding approach effectively models the probability of any subset of nodes forming a hyperlink by considering the latent positions of the hyperlink embedding and the center of their embeddings.

Example 2.2 (Distance-based generation on general manifolds). Consider \mathbf{x} valued on \mathbb{H} and $\mathcal{Z}_n \subset \mathbb{H}$, where \mathbb{H} is a general manifold. Let $d_{\mathbb{H}}(\mathbf{x}, \mathbf{z}_i)$ be the distance between \mathbf{x} and \mathbf{z}_i on \mathbb{H} . Consider $\mathbb{P}_{\mathcal{H}([n], \{E\})|\mathbf{x}, \mathcal{Z}_n, \alpha_n} (E = e) = \prod_{i \in e} p'_i(\mathbf{x}) \prod_{i \in [n] \setminus e} \{1 - p'_i(\mathbf{x})\}$, where $p'_i = g(-d_{\mathbb{H}}(\mathbf{x}, \mathbf{z}_i), \alpha_i)$ for some function $g : \mathbb{R} \times \mathbb{R} \rightarrow [0, 1]$ non-decreasing monotone in both its arguments. This embedding approach has been shown to effectively capture hierarchical geometry among graphical network nodes in hyperbolic latent spaces (Li et al. 2023). For denoising diffused embeddings on general manifolds, one can refer to the work in Huang et al. (2022).

Example 2.3 (Deterministic generation). Consider a deterministic function $f : \mathcal{X} \times \mathcal{Z}^n \times \mathbb{R}^n \rightarrow \mathcal{P}([n])$, where \mathcal{X} denotes the hyperlink embedding space and \mathcal{Z} denotes the node em-

bedding space with \mathcal{Z}^n being the product of n such spaces. Let $\mathbb{P}_{\mathcal{H}([n],\{E\})|\mathbf{x},\mathcal{Z}_n,\boldsymbol{\alpha}_n} = \delta_{f(\mathbf{x},\mathcal{Z}_n,\boldsymbol{\alpha}_n)}$ be a Dirac measure on $\mathcal{P}([n])$, concentrated at $f(\mathbf{x},\mathcal{Z}_n,\boldsymbol{\alpha}_n)$. Under this generation rule, hyperlink generation is deterministic once the embeddings \mathbf{x} , \mathcal{Z}_n , and $\boldsymbol{\alpha}_n$ are given. Such deterministic generation processes conditioned on the latent embeddings have been considered in [Li & Schramm \(2023\)](#) for community detection in block models.

Given a conditional likelihood hypergraph model, we need to estimate the latent embeddings from the observed hypergraph $\mathcal{H}([n],\mathcal{E}_m)$. We use [Example 2.1](#) to illustrate the estimation procedure. To proceed, we first need to address the identifiability issue of the model parameters in [Example 2.1](#). Note that for any $\boldsymbol{\mu}_{\mathbf{X}} \in \mathbb{R}^K$ and full rank $\mathbf{A} \in \mathbb{R}^{K \times K}$, by letting

$$\mathbf{X}' = \mathbf{A}^\top(\mathbf{X} - \boldsymbol{\mu}_{\mathbf{X}}), \mathbf{z}'_i = \mathbf{A}^{-1}\mathbf{z}_i, \text{ and } \alpha'_i = \alpha_i + \boldsymbol{\mu}_{\mathbf{X}}^\top\mathbf{z}_i, \text{ for } i \in [n], \quad (2.2)$$

we have $\sigma(\mathbf{X}^\top\mathbf{z}_i + \alpha_i) = \sigma(\mathbf{X}'^\top\mathbf{z}'_i + \alpha'_i)$ for all $i \in [n]$. This indicates that $\mathbb{P}_{\mathbf{X}}$ and \mathcal{Z}_n are identifiable up to a shift in $\mathbb{P}_{\mathbf{X}}$ and an invertible linear transformation between \mathbf{X} and $\{\mathbf{z}_1, \dots, \mathbf{z}_n\}$, as these transformations do not change the hyperlink distribution. To address this issue, we consider the following identifiability conditions on the hyperlink embedding distribution and the node embeddings: (C1) $\mathbb{E}_{\mathbb{P}_{\mathbf{X}}}[\mathbf{X}] = \mathbf{0}_K$, (C2) $\mathbb{E}_{\mathbb{P}_{\mathbf{X}}}[\mathbf{X}\mathbf{X}^\top] = \mathbf{Z}_n^\top\mathbf{Z}_n/n$ and both of them are diagonal, where $\mathbf{Z}_n = (\mathbf{z}_1, \dots, \mathbf{z}_n)^\top \in \mathbb{R}^{n \times K}$.

Remark 2.1. *The identifiability conditions (C1) and (C2) are for controlling the above shift issue in $\mathbb{P}_{\mathbf{X}}$ and the invertible linear transformation between \mathbf{X} and $\{\mathbf{z}_1, \dots, \mathbf{z}_n\}$, respectively, to guarantee the estimatibility of $\mathbb{P}_{\mathbf{X}}$, $\{\mathbf{z}_1, \dots, \mathbf{z}_n\}$, and $\boldsymbol{\alpha}_n$. Such identifiability conditions have been widely considered in the literature; see, for example, [Bai & Li \(2012\)](#), [Wang \(2022\)](#) and [Wu et al. \(2024\)](#). Another commonly used set of conditions is that $\mathbb{E}_{\mathbb{P}_{\mathbf{X}}} = \mathbf{0}_K$, $\mathbb{E}_{\mathbb{P}_{\mathbf{X}}}[\mathbf{X}\mathbf{X}^\top] = \mathbf{I}_K$, and $\mathbf{Z}_n^\top\mathbf{Z}_n/n$ is diagonal. These conditions can be transformed to (C1) and (C2) by multiplying $(\mathbf{Z}_n^\top\mathbf{Z}_n/n)^{-1/2}$ on \mathbf{X} and $(\mathbf{Z}_n^\top\mathbf{Z}_n/n)^{1/2}$ on each of $\{\mathbf{z}_1, \dots, \mathbf{z}_n\}$. We choose conditions (C1) and (C2) for technical purposes in the theoretical*

analysis. Similar theoretical results can also be derived for other identifiability conditions that guarantee the estimatibility of $\mathbb{P}_{\mathbf{X}}$, $\{\mathbf{z}_1, \dots, \mathbf{z}_n\}$, and $\boldsymbol{\alpha}_n$.

Remark 2.2. In general, if the true $\mathbb{P}_{\mathbf{X}}$ and \mathcal{Z}_n do not satisfy these constraints, a transformation of $\mathbb{P}_{\mathbf{X}}$, \mathcal{Z}_n , and $\boldsymbol{\alpha}_n$ can be made so that the constraints are met and the hyperlink distribution remains unchanged. In particular, let $\boldsymbol{\alpha}'_n = \boldsymbol{\alpha}_n + \mathbf{Z}_n \cdot \mathbb{E}_{\mathbb{P}_{\mathbf{X}}}[\mathbf{X}]$. We denote $\mathcal{V} = \text{diag}(\rho_1^2, \dots, \rho_K^2)$, with $\rho_1^2 > \rho_2^2 > \dots > \rho_K^2$ being the eigenvalues of $n^{-1}(\mathbf{Z}_n^\top \mathbf{Z}_n)^{1/2} \mathbb{E}_{\mathbb{P}_{\mathbf{X}}}[(\mathbf{X} - \mathbb{E}_{\mathbb{P}_{\mathbf{X}}}[\mathbf{X}])(\mathbf{X} - \mathbb{E}_{\mathbb{P}_{\mathbf{X}}}[\mathbf{X}])^\top] (\mathbf{Z}_n^\top \mathbf{Z}_n)^{1/2}$, and denote $\boldsymbol{\Gamma}$ as the $K \times K$ matrix whose columns collect the corresponding eigenvectors. Furthermore, let $\mathbf{X}' = \mathbf{G}^\top (\mathbf{X} - \mathbb{E}_{\mathbb{P}_{\mathbf{X}}}[\mathbf{X}])$ and $\mathbf{Z}'_n = \mathbf{Z}_n (\mathbf{G}^{-1})^\top$, where $\mathbf{G} = (\mathbf{Z}_n^\top \mathbf{Z}_n / n)^{1/2} \boldsymbol{\Gamma} \mathcal{V}^{-1/4}$. Then $\mathbb{P}_{\mathbf{X}'}$, \mathbf{Z}'_n and $\boldsymbol{\alpha}'_n$ will satisfy identifiability conditions (C1) and (C2), while keeping the hyperlink distribution unchanged. Another interpretation of the transformation is that we fix $\boldsymbol{\mu}_{\mathbf{X}} = \mathbb{E}_{\mathbb{P}_{\mathbf{X}}}[\mathbf{X}]$ and $\mathbf{A} = \mathbf{G}$ in (2.2).

Throughout this article, we assume that all the embeddings $\{\mathbf{z}_1, \dots, \mathbf{z}_n\}$ are bounded and $\mathbb{P}_{\mathbf{X}}$ is supported on a bounded set. Define $\bar{\alpha}_{m,n} = \sum_{i=1}^n \alpha_i / n$ to be the average node degree parameter. We assume that $|\alpha_i - \bar{\alpha}_{m,n}|$ is bounded for all $i \in [n]$ and $\bar{\alpha}_{m,n}$ is upper bounded but can diverge to $-\infty$ as $m, n \rightarrow \infty$. The expected degree of an hyperlink E is then

$$\mathbb{E}\left[\sum_{i=1}^n \mathbf{1}_{\{i \in E\}}\right] = \mathbb{E}_{\mathbb{P}_{\mathbf{X}}}\left[\sum_{i \in [n]} \frac{\exp(\mathbf{X}^\top \mathbf{z}_i + \alpha_i)}{1 + \exp(\mathbf{X}^\top \mathbf{z}_i + \alpha_i)}\right] \asymp n \exp(\bar{\alpha}_{m,n}),$$

as $m, n \rightarrow \infty$, which can be much smaller than n as $\bar{\alpha}_{m,n} \rightarrow -\infty$. This is consistent with the observation in hypergraph data that the orders of hyperlinks are usually much smaller compared with the total number of nodes. Theoretical analyses in Section 3 will further illustrate how the rate of $\exp(\bar{\alpha}_{m,n})$, i.e., the hyperlink sparsity, affects the performance of DDE. Accordingly, for an observed hypergraph $\mathcal{H}([n], \{e_1, \dots, e_m\})$, consider the log-likelihood function

$$\begin{aligned} \mathcal{L}(\mathcal{X}_m, \mathcal{Z}_n, \boldsymbol{\alpha}_n) &:= \mathcal{L}(\mathcal{H}([n], \{e_1, \dots, e_m\}) | \mathcal{X}_m, \mathcal{Z}_n, \boldsymbol{\alpha}_n) \\ &= \sum_{j=1}^m \sum_{i=1}^n \left\{ \mathbf{1}_{i \in e_j} (\mathbf{x}_j^\top \mathbf{z}_i + \alpha_i) - \log(1 + \exp(\mathbf{x}_j^\top \mathbf{z}_i + \alpha_i)) \right\} \end{aligned}$$

and the following constrained maximum likelihood estimator

$$\begin{aligned} \max_{\mathcal{X}_m, \mathcal{Z}_n, \boldsymbol{\alpha}_n} \mathcal{L}(\mathcal{X}_m, \mathcal{Z}_n, \boldsymbol{\alpha}_n) \quad \text{s.t.} \quad & \frac{1}{n} \mathbf{Z}_n^\top \mathbf{Z}_n = \frac{1}{m} \mathbf{X}_m^\top \mathbf{X}_m, \quad \mathbf{Z}_n^\top \mathbf{Z}_n \text{ and } \mathbf{X}_m^\top \mathbf{X}_m \text{ are diagonal,} \\ & \max\{\|\mathbf{Z}_n\|_{\max}, \|\mathbf{X}_m\|_{\max}, \|\boldsymbol{\alpha}_n - \frac{\sum_{i=1}^n \alpha_i}{n} \cdot \mathbf{1}_n\|_{\infty}\} \leq C, \quad (2.3) \\ & \text{and } -C_{m,n} \leq n^{-1} \sum_{i=1}^n \alpha_i \leq -C' C_{m,n}, \end{aligned}$$

for some constants $C > 0$, $C' \in (0, 1)$, and a boundary parameter $C_{m,n} > 0$ that can slowly diverge as $m, n \rightarrow \infty$ with $C_{m,n}$ serving to account for the hyperlink sparsity. We suggest to set $C_{m,n} = -C'' \log\{\sum_{j=1}^m |e_j|/(mn)\}$ for some $C'' > 1$ due to Proposition 3.2 in Wu et al. (2024). The constraints in (2.3) are from the identifiability conditions (C1) and (C2) by noticing that $\mathcal{X}_m = \{\mathbf{x}_1, \dots, \mathbf{x}_m\}$ are m realizations of $\mathbb{P}_{\mathbf{X}}$. Let $\hat{\mathcal{X}}_m = \{\hat{\mathbf{x}}_1, \dots, \hat{\mathbf{x}}_m\}$, $\hat{\mathcal{Z}}_n = \{\hat{\mathbf{z}}_1, \dots, \hat{\mathbf{z}}_n\}$ and $\hat{\boldsymbol{\alpha}}_n = (\hat{\alpha}_1, \dots, \hat{\alpha}_n)^\top$ be the solution to (2.3). We have now completed the first step in Algorithm 1.

Next, we introduce the second modeling part, the diffusion model architecture, from which we aim to generate new hyperlink embeddings. As the realizations from $\mathbb{P}_{\mathbf{X}}$ in \mathcal{X}_m are not observed, we achieve this by denoising diffused $\hat{\mathcal{X}}_m$ with a diffusion model architecture (Sohl-Dickstein et al. 2015, Song et al. 2020, Ho et al. 2020). A diffusion model consists of a forward process and a backward process. In the forward process, realizations from the target distribution are gradually perturbed by Gaussian random noise into pure noise. In the backward process, denoising neural networks are trained to remove the added noise and recover new realizations from the target distribution. There has been a long line of research on different ways to train a diffusion model and sample from it (Lu et al. 2022, Song et al. 2023). We consider a specific class of them in this paper. For forward process, we consider the Ornstein-Uhlenbeck process via the following Stochastic Differential Equation (SDE),

$$d\mathbf{X}_t = -\mathbf{X}_t dt + \sqrt{2} d\mathbf{W}_t, \quad (2.4)$$

where $(\mathbf{W}_t)_{t \geq 0}$ is a standard Wiener process. Suppose the forward process stops at time T . Under mild conditions, the resulting perturbed realizations for sufficiently large T will

be close to a standard multivariate Gaussian distribution. Diffusion models then generate new realizations from the target distribution by the reverse process

$$d\mathbf{X}_t^\leftarrow = \{\mathbf{X}_t^\leftarrow + 2\nabla \log p_{T-t}(\mathbf{X}_t^\leftarrow)\}dt + \sqrt{2}d\widetilde{\mathbf{W}}_t, \quad (2.5)$$

where $\nabla \log p_t(\cdot)$ is the score function, i.e., the gradient of the log probability density function of \mathbf{X}_t , and $\widetilde{\mathbf{W}}_t$ is another Wiener process independent of \mathbf{W}_t . The superscript “ \leftarrow ” is to distinguish the backward process from the forward process. Under mild conditions, when initialized with realizations from the distribution of \mathbf{X}_T , the backward process $(\mathbf{X}_t^\leftarrow)_{0 \leq t < T}$ shares the same distribution as the forward process $(\mathbf{X}_{T-t})_{0 \leq t < T}$.

However, directly sampling from (2.5) is unrealistic, as both the score functions and the distribution of \mathbf{X}_T are unknown. We replace the resulting distribution at time T in (2.4) with standard multivariate Gaussian distribution, discretizing the process with step size $h > 0$, and training deep neural networks to estimate the score functions, with the forward process initiated at $\{\hat{\mathbf{x}}_1, \dots, \hat{\mathbf{x}}_m\}$ on each trajectory. Specifically, consider $N = T/h$, which is the number of discretizations. Let s_{T-t} be the estimate of the score function $\nabla \log p_{T-t}$. For $t \in [kh, (k+1)h]$, the value of this estimate in the SDE is freezed at time kh . We sample from the SDE

$$d\mathbf{X}_t^\leftarrow = \{\mathbf{X}_t^\leftarrow + 2s_{T-kh}(\mathbf{X}_{kh}^\leftarrow)\}dt + \sqrt{2}d\widetilde{\mathbf{W}}_t \quad (2.6)$$

which initiates at samples from standard Gaussian distribution, to generate $\{\tilde{\mathbf{x}}_1, \dots, \tilde{\mathbf{x}}_{\tilde{m}}\}$. More details on the implementations of diffusion models are in the Supplementary Material.

Finally, let $\tilde{\mathcal{H}}_{\tilde{m},n} = \tilde{\mathcal{H}}([n], \{\tilde{E}_1, \dots, \tilde{E}_{\tilde{m}}\})$ denote a hypothetical random hypergraph, from which the hypergraph generated from Algorithm 1 is one realization. Given the estimated node embeddings $\hat{\mathcal{Z}}_n$, estimated node degree parameters $\hat{\alpha}_n$ and newly generated embeddings $\tilde{\mathcal{X}}_{\tilde{m}}$ from the diffusion model architecture trained on $\hat{\mathcal{X}}_m$, we generate $\tilde{\mathcal{H}}([n], \tilde{\mathcal{E}}_{\tilde{m}})$ based on $\mathbb{P}_{\tilde{\mathcal{H}}_{\tilde{m},n} | \tilde{\mathcal{X}}_{\tilde{m}}, \hat{\mathcal{Z}}_n, \hat{\alpha}_n} = \prod_{j=1}^{\tilde{m}} \mathbb{P}_{\mathcal{H}([n], \{\tilde{E}_j\}) | \mathbf{x}, \mathcal{Z}_n, \alpha_n}$.

Remark 2.3. *A straightforward approach to generate new hyperlinks is to sample directly from $\mathbb{P}_{\mathcal{H}_{m,n}|\hat{\mathbf{x}}_m, \hat{\mathbf{z}}_n, \hat{\boldsymbol{\alpha}}_n}$. However, this method can lead to privacy concerns. For instance, in the MIMIC-III dataset, each embedding $\hat{\mathbf{x}}_j$ represents profiling information about a patient and can be consistently estimated if new hyperlinks generated from this embedding are observed, as shown in Theorem 3.5 under linear generation processes. DDE aims to directly sample from $\mathbb{P}_{\mathbf{X}}$, avoiding leaking individual hyperlink information. The estimation of and sampling from $\mathbb{P}_{\mathbf{X}}$ are simultaneously achieved using the diffusion model architecture.*

3 Theoretical analysis

Our theoretical analysis in this section considers the following setup. The node embeddings $\mathcal{Z}_n = \{\mathbf{z}_1, \dots, \mathbf{z}_n\}$ and node degrees in $\boldsymbol{\alpha}_n = (\alpha_1, \dots, \alpha_n)^\top$ are treated as fixed parameters. The hyperlink embeddings $\mathcal{X}_m = \{\mathbf{x}_1, \dots, \mathbf{x}_m\}$ consist of m realizations drawn from the hyperlink embedding distribution $\mathbb{P}_{\mathbf{X}}$. The observed hypergraph is then generated from \mathcal{X}_m , \mathcal{Z}_n , and $\boldsymbol{\alpha}_n$, based on the conditional distribution $\mathbb{P}_{\mathcal{H}_{m,n}|\mathcal{X}_m, \mathcal{Z}_n, \boldsymbol{\alpha}_n}$, which can be decomposed into independent hyperlink generation processes: $\mathbb{P}_{\mathcal{H}_{m,n}|\mathcal{X}_m, \mathcal{Z}_n, \boldsymbol{\alpha}_n} = \prod_{j=1}^m \mathbb{P}_{\mathcal{H}([n], (E_j))|\mathbf{x}_j, \mathcal{Z}_n, \boldsymbol{\alpha}_n}$. Our goal is to evaluate how “close” the distribution of the hyperlinks generated by DDE (Algorithm 1) is to the distribution of hyperlinks generated by the true model, i.e., by $\mathbb{P}_{\mathbf{X}}$ and $\mathbb{P}_{\mathcal{H}([n], \{E\})|\mathbf{X}, \mathcal{Z}_n, \boldsymbol{\alpha}_n}$. We begin in Section 3.1 with an initial study under the deterministic generation process in Example 2.3 and proceed to a detailed study under a non-deterministic generation process in Section 3.2.

3.1 An initial study under deterministic generation processes

We begin with a simplified version of the DDE algorithm. In the standard DDE setup, the hyperlink embeddings, node embeddings, and node degree parameters are all unknown and must be estimated from the observed hypergraph $\mathcal{H}([n], \mathcal{E}_m)$. However, if these embeddings

and node degrees are available, we can replace $\hat{\mathcal{X}}_m$, $\hat{\mathcal{Z}}_n$, and $\hat{\boldsymbol{\alpha}}_n$ in Algorithm 1 with \mathcal{X}_m , \mathcal{Z}_n , and $\boldsymbol{\alpha}_n$ that generate the hypergraph $\mathcal{H}([n], \mathcal{E}_m)$. Under this scenario, we can establish the following theorem.

Theorem 3.1. *Suppose $\hat{\mathcal{X}}_m$, $\hat{\mathcal{Z}}_n$ and $\hat{\boldsymbol{\alpha}}_n$ in Algorithm 1 are replaced with \mathcal{X}_m , \mathcal{Z}_n and $\boldsymbol{\alpha}_n$, respectively. Let \mathbb{P}_E , $\mathbb{P}_{\tilde{E}}$, $\mathbb{P}_{\mathbf{X}}$ and $\mathbb{P}_{\tilde{\mathbf{X}}}$ denote the marginal distributions of hyperlinks generated by the true model, hyperlinks generated by DDE, the true hyperlink embeddings, and the hyperlink embeddings generated from diffusion models trained on \mathcal{X}_m , respectively. Consider the deterministic generation process in Example 2.3 with any $f : \mathcal{X} \times \mathcal{Z}^n \times \mathbb{R}^n \rightarrow \mathcal{P}([n])$. We have $d_{\text{TV}}(\mathbb{P}_E, \mathbb{P}_{\tilde{E}}) \leq d_{\text{TV}}(\mathbb{P}_{\mathbf{X}}, \mathbb{P}_{\tilde{\mathbf{X}}})$.*

Theorem 3.1 demonstrates that when \mathcal{X}_m , \mathcal{Z}_n , and $\boldsymbol{\alpha}_n$ are available for use in DDE, the total variation distance between the distributions of hyperlinks generated from the true model and those generated by DDE is upper bounded by the total variation distance between the distributions of hyperlink embeddings generated from the true model and those generated by the diffusion model trained on \mathcal{X}_m . This implies that, under a deterministic generation rule with \mathcal{X}_m , \mathcal{Z}_n , and $\boldsymbol{\alpha}_n$ available, DDE reduces the generative error for a high-dimensional discrete distribution to that of a low-dimensional continuous distribution. In real-world scenarios, however, \mathcal{X}_m , \mathcal{Z}_n , and $\boldsymbol{\alpha}_n$ are not directly available and must be estimated from the observed hypergraph. We defer the discussion of such cases under a non-deterministic generation process to Section 3.2.

Next, we study an example from Chen, Huang, Zhao & Wang (2023) that considers generative modeling for data supported on a low-dimensional manifold, which has a close connection to our setup under deterministic hyperlink generation processes.

Example 3.2 (Generating continuous vectors residing on low-dimensional spaces in Chen, Huang, Zhao & Wang (2023)). *Suppose that we observe m vectors of dimension n in $\{\mathbf{y}_j\}_{j \in [m]} \subset \mathbb{R}^n$ residing on a low-dimensional linear subspace: each \mathbf{y}_j can be expressed*

as $\mathbf{Z}\mathbf{x}_j$, where $\mathbf{Z} \in \mathbb{R}^{n \times K}$ is an unknown matrix with orthonormal columns, i.e. $\mathbf{Z}^\top \mathbf{Z} = \mathbf{I}_K$, and latent vectors \mathbf{x}_j are independently and identically distributed from some distribution $\mathbb{P}_{\mathbf{X}}$. The goal is to generate new samples of \mathbf{y} 's.

Notice that a random subset of $[n]$ can be encoded as a random binary vector valued in $\{0, 1\}^n$, where the coordinates of 1's indicate the indices included in the subset. Generating hyperlinks can thus be viewed as generating n -dimensional vectors valued in a discrete space $\{0, 1\}^n$, while Example 3.2 aims to generate n -dimensional vectors valued in a continuous space \mathbb{R}^n . Both our work and Example 3.2 consider a low-dimensional structure on the data. Specifically, in Example 3.2, a deterministic generation process of \mathbf{y}_j is considered given the latent vector \mathbf{x}_j : $\mathbf{y}_j = \mathbf{Z}\mathbf{x}_j$. Chen, Huang, Zhao & Wang (2023) proposed leveraging this low-dimensional structure by modifying the structure of the score network in the diffusion model during the score estimation procedure. They theoretically demonstrate that such modifications help diffusion models to circumvent the curse of ambient dimensionality of data points. Alternatively, this low-dimensional structure can be exploited using DDE. Instead of considering a conditional distribution $\mathbb{P}_{\mathcal{H}([n], E) | \mathbf{X}, \mathbf{Z}_n}$ for a hyperlink, we consider the deterministic generation process $\mathbf{y}_j = \mathbf{Z}\mathbf{x}_j$ for all $j \in [m]$, with an unknown orthonormal matrix $\mathbf{Z} \in \mathbb{R}^{n \times K}$. We design a modified DDE algorithm in Algorithm 2 for Example 3.2 and study in Corollary 3.1 the theoretical property of its output.

Corollary 3.1. *Let $\mathbb{P}_{\mathbf{Y}}$ denote the true distribution of \mathbf{Y} in Example 3.2 and let $\mathbb{P}_{\tilde{\mathbf{Y}}}$ denote the distribution of generated ones by Algorithm 2. Let $\mathbb{P}_{\mathbf{X}\Gamma}$ denote the distribution of \mathbf{X} after an orthogonal transformation Γ , and $\mathbb{P}_{\widehat{\mathbf{X}\Gamma}}$ denote the distribution of the vectors generated from the diffusion model trained on m realizations of $\mathbb{P}_{\mathbf{X}\Gamma}$. Then there exists a K -dimensional orthogonal transformation such that*

$$d_{\text{TV}}(\mathbb{P}_{\mathbf{Y}}, \mathbb{P}_{\tilde{\mathbf{Y}}}) \leq d_{\text{TV}}(\mathbb{P}_{\mathbf{X}\Gamma}, \mathbb{P}_{\widehat{\mathbf{X}\Gamma}}).$$

Corollary 3.1 demonstrates that the modified DDE can exactly circumvent the curse

Algorithm 2: Modified DDE for Example 3.2.

Input: $\mathbf{Y} = (\mathbf{y}_1, \dots, \mathbf{y}_m)^\top \in \mathbb{R}^{m \times n}$; Diffusion model architecture \mathcal{M} ; Latent space dimension K .

- 1 *Latent space embedding recovery:* Conduct top- K singular value decomposition on \mathbf{Y} and get $\mathbf{Y} = \mathbf{U}\mathbf{\Sigma}\mathbf{V}^\top$, where $\mathbf{U} \in \mathbb{R}^{m \times K}$ and $\mathbf{V} \in \mathbb{R}^{n \times K}$ satisfy $\mathbf{U}^\top \mathbf{U} = \mathbf{I}$, and $\mathbf{\Sigma}$ is the diagonal matrix of the K singular values. Let $\hat{\mathbf{Z}} = \mathbf{V}$ and $(\hat{\mathbf{x}}_1, \dots, \hat{\mathbf{x}}_m)^\top = \mathbf{U}\mathbf{\Sigma}$.
- 2 *Diffusion models on the embeddings:* Train the diffusion model architecture \mathcal{F} on $\{\hat{\mathbf{x}}_1, \dots, \hat{\mathbf{x}}_m\}$ to get a sampler $\hat{\mathcal{M}}$ and sample \tilde{m} embeddings $\tilde{\mathcal{X}}_{\tilde{m}} = \{\tilde{\mathbf{x}}_1, \dots, \tilde{\mathbf{x}}_m\}$ from $\hat{\mathcal{M}}$.
- 3 *Generating \mathbf{y} from the embeddings:* Let $\tilde{\mathbf{y}}_j = \hat{\mathbf{Z}}\tilde{\mathbf{x}}_j$ for $j \in [\tilde{m}]$.

Output: $\{\tilde{\mathbf{y}}_1, \dots, \tilde{\mathbf{y}}_{\tilde{m}}\}$.

of ambient dimensionality of data points under the setup in [Chen, Huang, Zhao & Wang \(2023\)](#). The study of the convergence of diffusion models in the low-dimensional space is deferred to Section 3.3.

3.2 Theoretical analysis for DDE under a non-deterministic generation process

Now we consider a non-deterministic generation process. We first present a general theorem on DDE under the assumption that the true embeddings and parameters are available. Let $\mathbb{P}_{(E, \mathbf{X})}$ denote the joint distribution of a hyperlink E and its associated hyperlink embedding \mathbf{X} . Let $\mathbb{P}_{\tilde{\mathbf{X}}}$ denote the marginal distribution of a hyperlink embedding $\tilde{\mathbf{X}}$ sampled from diffusion models trained on $\{\mathbf{x}_1, \dots, \mathbf{x}_m\}$. Additionally, let $\mathbb{P}_{(\tilde{E}, \tilde{\mathbf{X}})}$ denote the joint distribution of $\tilde{\mathbf{X}}$ and a hyperlink generated from this embedding along with \mathcal{Z}_n and $\boldsymbol{\alpha}_n$. We establish the following lemma.

Lemma 3.1. $d_{\text{KL}}(\mathbb{P}_{(E, \mathbf{X})} \| \mathbb{P}'_{(\tilde{E}, \tilde{\mathbf{X}})}) = d_{\text{KL}}(\mathbb{P}_{\mathbf{X}} \| \mathbb{P}'_{\tilde{\mathbf{X}}})$.

Lemma 3.1 demonstrates that DDE reduces the generative error for high-dimensional hyperlinks to the generative error for low-dimensional hyperlink embeddings under the ideal scenario where \mathcal{X}_m , \mathcal{Z}_n , and $\boldsymbol{\alpha}_n$ are available. In cases where the embeddings and node degrees must be estimated, we introduce the distributions $\mathbb{P}'_{(\tilde{E}, \tilde{\mathbf{X}})}$ and $\mathbb{P}'_{\tilde{\mathbf{X}}}$.

Definition 3.3. *Conditioned on \mathcal{X}_m , we use $\mathbb{P}'_{(\tilde{E}, \tilde{\mathbf{X}})}$ to denote a random measure on the joint distribution of a generated hyperlink embedding $\tilde{\mathbf{X}}$ and the hyperlink \tilde{E} generated from $\tilde{\mathbf{X}}$, $\hat{\mathcal{Z}}_n$ and $\hat{\boldsymbol{\alpha}}_n$. More formally, this random measure should be denoted by $\mathbb{P}'_{(\tilde{E}, \tilde{\mathbf{X}}) | \hat{\mathcal{X}}_m, \hat{\mathcal{Z}}_n, \hat{\boldsymbol{\alpha}}_n}$, and here we use the notation $\mathbb{P}'_{(\tilde{E}, \tilde{\mathbf{X}})}$ for simplicity. The distribution of this random measure depends on the m realizations of hyperlink embeddings \mathcal{X}_m . The randomness in $\mathbb{P}'_{(\tilde{E}, \tilde{\mathbf{X}})}$ is from the hypergraph generation process given \mathcal{X}_m , \mathcal{Z}_n and $\boldsymbol{\alpha}_n$, which introduces randomness in the estimated embeddings $\hat{\mathcal{X}}_m$, $\hat{\mathcal{Z}}_n$ and node degrees $\hat{\boldsymbol{\alpha}}_n$, thus leading to randomness in the distribution of $\tilde{\mathbf{X}}$ and \tilde{E} . Similarly, $\mathbb{P}'_{\tilde{\mathbf{X}}} := \mathbb{P}'_{\tilde{\mathbf{X}} | \hat{\mathcal{X}}_m, \hat{\mathcal{Z}}_n, \hat{\boldsymbol{\alpha}}_n}$ is a random measure on $\tilde{\mathbf{X}}$ conditioned on \mathcal{X}_m .*

The following theorem decomposes the distance between $\mathbb{P}_{(E, \mathbf{X})}$ and $\mathbb{P}'_{(\tilde{E}, \tilde{\mathbf{X}})}$.

Theorem 3.4. *The KL-divergence between $\mathbb{P}_{(E, \mathbf{X})}$ and $\mathbb{P}'_{(\tilde{E}, \tilde{\mathbf{X}})}$ can be decomposed into three terms as follows:*

$$d_{\text{KL}}(\mathbb{P}_{(E, \mathbf{X})} \| \mathbb{P}'_{(\tilde{E}, \tilde{\mathbf{X}})}) = \text{error}_{(\mathbf{z}, \boldsymbol{\alpha})\text{-estimation}} + \text{error}_{\mathbb{P}_{\mathbf{X}}\text{-estimation}} + \text{error}_{\text{diffusion}}.$$

Specifically, the three terms takes the following forms:

$$\begin{aligned}
\text{error}_{(\mathbf{z}, \alpha)\text{-estimation}} &= \mathbb{E}_{\mathbb{P}_{(E, \mathbf{X})}} \left[\log \left\{ \frac{d\mathbb{P}_{\mathcal{H}([n], \{E\}) | \mathbf{X}, \mathcal{Z}_n, \alpha_n}(E, \mathbf{X})}{d\mu(\mathcal{H}([n], \{E\}))} \right\} \right], \\
\text{error}_{\mathbb{P}_{\mathbf{X}}\text{-estimation}} &= \mathbb{E}_{\mathbb{P}_{\mathbf{X}}} \left[\log \left\{ \frac{d\mathbb{P}_{\mathbf{X}}(\mathbf{X})}{d\mu(\hat{\mathbf{X}})}(\mathbf{X}) \right\} \right] + \mathbb{E}_{\mathbb{P}_{\mathbf{X}}} \left[\log \left\{ \frac{d\mathbb{P}_{\hat{\mathbf{X}}_m}(\mathbf{X})}{d\mu(\hat{\mathbf{X}})}(\mathbf{X}) \right\} \right] \\
&\quad - \mathbb{E}_{\mathbb{P}_{\hat{\mathbf{X}}_m}} \left[\log \left\{ \frac{d\mathbb{P}_{\hat{\mathbf{X}}_m}(\mathbf{X})}{d\mu(\hat{\mathbf{X}})}(\mathbf{X}) \right\} \right], \text{ and} \\
\text{error}_{\text{diffusion}} &= \mathbb{E}_{\mathbb{P}_{\hat{\mathbf{X}}_m}} \left[\log \left\{ \frac{d\mathbb{P}_{\hat{\mathbf{X}}_m}(\mathbf{X})}{d\mu(\hat{\mathbf{X}})}(\mathbf{X}) \right\} \right],
\end{aligned}$$

where $\mathbb{P}_{\hat{\mathbf{X}}_m}$ stands for the marginal distribution of each one of $\{\hat{\mathbf{x}}_1, \dots, \hat{\mathbf{x}}_m\}$ given \mathcal{X}_m and we assume absolute continuity of the log ratios without loss of generality.

The first term in Theorem 3.4 is referred to as $\text{error}_{(\mathbf{z}, \alpha)\text{-estimation}}$ since $\frac{d\mathbb{P}_{\mathcal{H}([n], \{E\}) | \mathbf{X}, \mathcal{Z}_n, \alpha_n}(E, \mathbf{X})}{d\mu(\mathcal{H}([n], \{E\}))}$ and $\frac{d\mathbb{P}_{\mathcal{H}([n], \{\bar{E}\}) | \bar{\mathbf{X}}, \hat{\mathcal{Z}}_n, \hat{\alpha}_n}(E, \mathbf{X})}{d\mu(\mathcal{H}([n], \{\bar{E}\}))}$ only differ in $\hat{\mathcal{Z}}_n$ and $\hat{\alpha}_n$ with the same plugged-in (E, \mathbf{X}) pairs. The second term, $\text{error}_{\mathbb{P}_{\mathbf{X}}\text{-estimation}}$, is so named because it primarily depends on the distance between $\mathbb{P}_{\mathbf{X}}$ and $\mathbb{P}_{\hat{\mathbf{X}}_m}$. The third term $\text{error}_{\text{diffusion}}$ quantifies the error in generating observations of $\mathbb{P}_{\hat{\mathbf{X}}_m}$ using diffusion models. We analyze the three terms in sequence.

Consider the linear embedding approach in Example (2.1), and that $\mathbb{P}_{\mathbf{X}}$, \mathcal{Z}_n , and α_n satisfy the identifiability conditions (C1) and (C2). We analyze $\text{error}_{(\mathbf{z}, \alpha)\text{-estimation}}$ and $\text{error}_{\mathbb{P}_{\mathbf{X}}\text{-estimation}}$ under an asymptotic regime where both m and n go to infinity and consider the following conditions.

Condition 3.1 (Embedding assumptions). *The node embeddings and degrees satisfy $\max\{\max_{i \in [n]} \|\mathbf{z}_i\|_\infty, \max_{i \in [n]} |\alpha_i - \sum_{i=1}^n \alpha_i/n|\} \leq C$ for the constant C in (2.3) and also the support of $\mathbb{P}_{\mathbf{X}}$ satisfies $\text{supp}(\mathbb{P}_{\mathbf{X}}) \subset \{\mathbf{x} \in \mathbb{R}^K : \|\mathbf{x}\|_\infty \leq C\}$. For the m realizations of $\mathbb{P}_{\mathbf{X}}$ collected in \mathcal{X}_m , they satisfy that $\|m^{-1} \sum_{j=1}^m \mathbf{x}_j\|_2 = O(\{(m \wedge n) \exp(\bar{\alpha}_{m,n})\}^{-1/2})$ and $\|\mathbf{X}_m^\top \mathbf{X}_m/m - \mathbb{E}_{\mathbb{P}_{\mathbf{X}}}[\mathbf{X}\mathbf{X}^\top]\|_2 = O(\{(m \wedge n) \exp(\bar{\alpha}_{m,n})\}^{-1})$. The minimum eigenvalue of*

$\mathbb{E}_{\mathbb{P}_{\mathbf{X}}}[\mathbf{X}\mathbf{X}^\top]$ is lower bounded by a constant, and eigenvalues of $\mathbb{E}_{\mathbb{P}_{\mathbf{X}}}[\mathbf{X}\mathbf{X}^\top]$ are distinct and their gaps are lower bounded by a constant.

Condition 3.2 (Hyperlink sparsity assumptions). *The average node degree parameter $\bar{\alpha}_{m,n}$ satisfies that $\exp(\bar{\alpha}_{m,n}) \gtrsim (m \vee n)^{\epsilon^*} / (m \wedge n)$ for some arbitrarily small $\epsilon^* > 0$.*

Condition 3.1 assumes bounded embeddings and degree heterogeneity, and a reasonable convergence rate of the first and second moments of \mathcal{X}_m to their population counterparts. Notably, for sparser hypergraphs, the required rate of this convergence is less stringent. Condition 3.2 specifies the minimum expected hyperlink order requirement, which is $n(m \vee n)^{\epsilon^*} / (m \wedge n)$ for some small $\epsilon^* > 0$. Under these conditions, we have the following Theorem 3.5 which will be used in analyzing $\text{error}_{(\mathbf{z}, \alpha)\text{-estimation}}$ and $\text{error}_{\mathbb{P}_{\mathbf{X}}\text{-estimation}}$.

Theorem 3.5. *Let $\mathbf{x}_1, \dots, \mathbf{x}_m$ be m realizations from $\mathbb{P}_{\mathbf{X}}$ and $\mathcal{H}([n], \mathcal{E}_m)$ be generated from $\mathcal{X}_m = \{\mathbf{x}_1, \dots, \mathbf{x}_m\}$, $\mathcal{Z}_n = \{\mathbf{z}_1, \dots, \mathbf{z}_n\}$ and $\boldsymbol{\alpha}_n = (\alpha_1, \dots, \alpha_n)^\top$. Let $\hat{\mathcal{X}}_m = \{\hat{\mathbf{x}}_1, \dots, \hat{\mathbf{x}}_m\}$, $\hat{\mathcal{Z}}_n = \{\hat{\mathbf{z}}_1, \dots, \hat{\mathbf{z}}_n\}$ and $\hat{\boldsymbol{\alpha}} = (\hat{\alpha}_1, \dots, \hat{\alpha}_n)^\top$ be the solution to (2.3), where we set $C_{m,n} = -C''' \log\{\sum_{j=1}^m |e_j| / (mn)\}$ for some $C''' > 1$. Suppose Conditions 3.1 and 3.2 hold. Then for any $\epsilon > 0$, we have*

$$\max \left\{ \max_{j \in [m]} \|\hat{\mathbf{x}}_j - \mathbf{x}_j\|_\infty, \max_{i \in [n]} \|\hat{\mathbf{z}}_i - \mathbf{z}_i\|_\infty, \max_{i \in [n]} |\hat{\alpha}_i - \alpha_i| \right\} = O_p \left\{ \frac{(m \vee n)^\epsilon}{(m \wedge n)^{\frac{1}{2}} \exp(\bar{\alpha}_{m,n}/2)} \right\}$$

as $m, n \rightarrow \infty$.

Building on Theorem 3.5, we have the rate for $\text{error}_{(\mathbf{z}, \alpha)\text{-estimation}}$ as follows.

Theorem 3.6. *Consider the linear embedding approach in Example 2.1. Suppose that Condition 3.1 holds. Then for any $\epsilon > 0$, we have*

$$\frac{1}{n} \text{error}_{(\mathbf{z}, \alpha)\text{-estimation}} = O_p \left\{ \frac{(m \vee n)^\epsilon}{(m \wedge n) \exp(\bar{\alpha}_{m,n})} \right\},$$

as $m, n \rightarrow \infty$. Then randomness in O_p is from realizations of hypergraphs given \mathcal{X}_m , \mathcal{Z}_n and $\boldsymbol{\alpha}_n$.

The analysis of $\text{error}_{\mathbb{P}_{\mathbf{X}}\text{-estimation}}$ is challenging, as it involves comparing the distribution of estimators for the m discrete realizations of $\mathbb{P}_{\mathbf{X}}$ in \mathcal{X}_m with the continuous distribution $\mathbb{P}_{\mathbf{X}}$. We use a discretization strategy to understand this error term.

Consider a discrete version \mathbf{X}^{dis} of \mathbf{X} with probability mass function $p_{\mathbf{X}^{\text{dis}}} = d\mathbb{P}_{\mathbf{X}^{\text{dis}}}/d\mu(\mathbf{X}^{\text{dis}})$ deduced by $p_{\mathbf{X}} := d\mathbb{P}_{\mathbf{X}}/d\mu(\mathbf{X})$ and a $\{C, \gamma_{m,n}^{-1}\}$ -grid:

$$\mathcal{A}_{C, \gamma_{m,n}^{-1}} = \{\mathbf{a} \in \mathbb{R}^K : \|\mathbf{a}\|_{\infty} \leq C, a_i \in 1/\gamma_{m,n} \cdot \mathbb{Z}, \text{ for } i = 1, \dots, K\},$$

where \mathbb{Z} is the collection of all integers and $\gamma_{m,n}$ is a sequence diverging to ∞ as $m, n \rightarrow \infty$.

The probability mass of each $\mathbf{x}^{\text{dis}} \in \mathcal{A}_{C, \gamma_{m,n}^{-1}}$ is then

$$p_{\mathbf{X}^{\text{dis}}}(\mathbf{x}^{\text{dis}}) = \int_{[\mathbf{x}^{\text{dis}} - \frac{1}{2\gamma_{m,n}}, \mathbf{x}^{\text{dis}} + \frac{1}{2\gamma_{m,n}}) \cap \text{supp}(\mathbb{P}_{\mathbf{X}})} p_{\mathbf{X}}(\mathbf{x}) d\mu(\mathbf{x}),$$

where $[\mathbf{x}^{\text{dis}} - \frac{1}{2\gamma_{m,n}}, \mathbf{x}^{\text{dis}} + \frac{1}{2\gamma_{m,n}})$ is a left-close-right-open hypercube with length $\frac{1}{\gamma_{m,n}}$ centered around \mathbf{x}^{dis} . $\mathbb{P}_{\mathbf{X}}$ and $\mathbb{P}_{\mathbf{X}^{\text{dis}}}$ are not directly comparable as they are defined on different sample spaces. To proceed, we induce a random vector \mathbf{X}^{pc} valued on the same sample space as \mathbf{X} from \mathbf{X}^{dis} , whose probability density function is piecewise constant. Without loss of generality, consider $\text{supp}(\mathbb{P}_{\mathbf{X}})$ to be perfectly divided by the $\{C, 1/\gamma_{m,n}\}$ -grid: $\text{supp}(\mathbb{P}_{\mathbf{X}}) = [-C - (2\gamma_{m,n})^{-1}, C + (2\gamma_{m,n})^{-1})$ and $\gamma_{m,n}$ are chosen so that $C/\gamma_{m,n} \in \mathbb{Z}$, where $[-C - (2\gamma_{m,n})^{-1}, C + (2\gamma_{m,n})^{-1})$ is the left-close-right-open hypercube centered at $\mathbf{0}$ with length $2C + (\gamma_{m,n})^{-1}$ on each coordinate. Let $\mathbb{P}_{\mathbf{X}^{\text{pc}}}$ be the distribution on $\text{supp}(\mathbb{P}_{\mathbf{X}})$ defined as follows: for any $\mathbf{x} \in \text{supp}(\mathbb{P}_{\mathbf{X}})$, let $\mathbf{x}^{\text{dis}}(\mathbf{x}) \in \mathcal{A}_{C, \gamma_{m,n}^{-1}}$ be such that $\mathbf{x} \in [\mathbf{x}^{\text{dis}}(\mathbf{x}) - (2\gamma_{m,n})^{-1}, \mathbf{x}^{\text{dis}}(\mathbf{x}) + (2\gamma_{m,n})^{-1})$; then

$$p_{\mathbf{X}^{\text{pc}}}(\mathbf{x}) := \frac{d\mathbb{P}_{\mathbf{X}^{\text{pc}}}}{d\mu(\mathbf{X}^{\text{pc}})}(\mathbf{x}) = \gamma_{m,n}^K \int_{[\mathbf{x}^{\text{dis}}(\mathbf{x}) - \frac{1}{2\gamma_{m,n}}, \mathbf{x}^{\text{dis}}(\mathbf{x}) + \frac{1}{2\gamma_{m,n}})} p_{\mathbf{X}}(\mathbf{x}) d\mu(\mathbf{x}).$$

Lemma 3.2. $p_{\mathbf{X}^{\text{pc}}}(\mathbf{x})$ is a probability density function.

Given that $p_{\mathbf{X}^{\text{pc}}}(\mathbf{x})$ is a proper probability density function as established in Lemma 3.2, the following theorem demonstrates a uniform distance bound between $p_{\mathbf{X}^{\text{pc}}}$ and $p_{\mathbf{X}}(\mathbf{x})$, which characterizes the distance bound between the distributions $\mathbb{P}_{\mathbf{X}^{\text{pc}}}$ and $\mathbb{P}_{\mathbf{X}}$.

Theorem 3.7. *Suppose $p_{\mathbf{X}}$ is L -Lipschitz continuous: for any $\mathbf{x}, \mathbf{x}' \in \text{supp}(\mathbb{P}_{\mathbf{X}})$, $|p_{\mathbf{X}}(\mathbf{x}) - p_{\mathbf{X}}(\mathbf{x}')| \leq L \cdot \|\mathbf{x} - \mathbf{x}'\|$. Then we have $|p_{\mathbf{X}^{\text{pc}}}(\mathbf{x}) - p_{\mathbf{X}}(\mathbf{x})| \leq L\sqrt{K}\gamma_{m,n}^{-1}, \forall \mathbf{x} \in \text{supp}(\mathbb{P}_{\mathbf{X}})$.*

Another common strategy to compare a continuous distribution with its discretized version is through kernel smoothing, which projects the discretized distribution to a continuous distribution with a smooth density. Since we do not need a smooth projection of $\mathbb{P}_{\mathbf{X}^{\text{dis}}}$ here to understand the difference between $\mathbb{P}_{\mathbf{X}}$ and $\mathbb{P}_{\mathbf{X}^{\text{dis}}}$, the piecewise constant version $\mathbb{P}_{\mathbf{X}^{\text{pc}}}$ suffices.

Since $\mathbb{P}'_{(\tilde{E}, \tilde{\mathbf{X}})}$ is defined conditioning on \mathcal{X}_m , we introduce $\mathbb{P}_{\mathcal{X}_m^{\text{dis}}}$, which is the empirical distribution of m realizations from $\mathbb{P}_{\mathbf{X}^{\text{dis}}}$. Let $\mathcal{X}_m^{\text{dis}} = \{\mathbf{x}_1^{\text{dis}}, \dots, \mathbf{x}_m^{\text{dis}}\}$, $\mathbb{P}_{\mathcal{X}_m^{\text{dis}}}$ has probability mass function

$$p_{\mathcal{X}_m^{\text{dis}}}(\mathbf{x}) = \frac{\# \text{ of } \mathbf{x} \text{ in } \mathcal{X}_m^{\text{dis}}}{m}, \forall \mathbf{x} \in \mathcal{A}_{C, \gamma_{m,n}^{-1}}.$$

The next lemma demonstrates the distance between the distribution of $\mathbb{P}_{\mathbf{X}^{\text{dis}}}$ and the empirical distribution $\mathbb{P}_{\mathcal{X}_m^{\text{dis}}}$ of m realizations of it.

Lemma 3.3. *Consider \mathcal{X}_m as a collection of m realizations of $\mathbb{P}_{\mathbf{X}^{\text{dis}}}$. For any $\epsilon_{m,n}$ satisfying that $\epsilon_{m,n} \gg \sqrt{K \log(2C\gamma_{m,n})/m}$ as $m, n \rightarrow \infty$, we have $\mathbb{P}\{\forall \mathbf{x} \in \mathcal{A}_{C, \gamma_{m,n}^{-1}}, |p_{\mathbf{X}^{\text{dis}}}(\mathbf{x}) - p_{\mathcal{X}_m^{\text{dis}}}(\mathbf{x})| \leq \epsilon_{m,n}\} \rightarrow 1$ as $m, n \rightarrow \infty$. The randomness argument comes from realizations of $\mathbb{P}_{\mathbf{X}^{\text{dis}}}$.*

When \mathcal{X}_m is replaced with $\mathcal{X}_m^{\text{dis}}$, the estimators from (2.3) need to be refined accordingly. We project the estimators $\{\hat{\mathbf{x}}_1, \dots, \hat{\mathbf{x}}_m\}$ onto $\mathcal{A}_{C, \gamma_{m,n}^{-1}}$. Let $\hat{\mathbf{x}}_j^{\text{dis}} = \text{argmin}_{\mathbf{x} \in \mathcal{A}_{C, \gamma_{m,n}^{-1}}} \|\mathbf{x} - \hat{\mathbf{x}}_j\|$. Then $\{\hat{\mathbf{x}}_1^{\text{dis}}, \dots, \hat{\mathbf{x}}_m^{\text{dis}}\}$ would have a probability mass function

$$p_{\hat{\mathcal{X}}_m^{\text{dis}}}(\mathbf{x}) = \frac{\# \text{ of } \mathbf{x} \text{ in } \hat{\mathcal{X}}_m^{\text{dis}}}{m}.$$

Theorem 3.8. *Consider the linear embedding approach in Example 2.1 and $\hat{\mathcal{X}}_m^{\text{dis}} = \{\hat{\mathbf{x}}_1^{\text{dis}}, \dots, \hat{\mathbf{x}}_m^{\text{dis}}\}$ as projections onto $\mathcal{A}_{C, \gamma_{m,n}^{-1}}$ of $\{\hat{\mathbf{x}}_1, \dots, \hat{\mathbf{x}}_m\}$ from (2.3). Suppose that Condition 3.1 holds and that $\gamma_{m,n} = o\{\exp(\bar{\alpha}_{m,n}/2)(m \wedge n)^{\frac{1}{2}-\epsilon}\}$ for some arbitrarily small $\epsilon > 0$. Then we have*

$\mathbb{P}(\forall j \in [m], \hat{\mathbf{x}}_j^{\text{dis}} = \mathbf{x}_j^{\text{dis}}) \rightarrow 1$, as $m, n \rightarrow \infty$. Consequently, $\mathbb{P}\{\forall \mathbf{x} \in \mathcal{A}_{C, \gamma_{m,n}^{-1}}, p_{\mathcal{X}_m^{\text{dis}}}(\mathbf{x}) = p_{\hat{\mathcal{X}}_m^{\text{dis}}}(\mathbf{x})\} \rightarrow 1$ as $m, n \rightarrow \infty$. The randomness comes from realizations of hypergraphs.

The above analysis shows that the marginal distribution of one point from $\hat{\mathcal{X}}_m^{\text{dis}}$ is close to $\mathbb{P}_{\mathbf{X}^{\text{dis}}}$. Moreover, combined with the results in Wu et al. (2024), this analysis indicates that $\mathbb{P}_{\mathbf{X}}$ and $\mathbb{P}_{\hat{\mathcal{X}}_m}$ are close, and $\{\hat{\mathbf{x}}_1, \dots, \hat{\mathbf{x}}_m\}$ are asymptotically independent. We then understand $\text{error}_{\text{diffusion}}$ via the distance between $\mathbb{P}_{\mathbf{X}}$ and the distribution of output of diffusion models trained on m realizations from $\mathbb{P}_{\mathbf{X}}$.

3.3 Convergence of the diffusion models

Consider sampling from the SDE (2.6). We are interested in $\epsilon_{\text{distribution}}$, defined as the distance between the distribution of outputs from the sampler and the target distribution, as for example measured using metrics such as KL divergence (Benton et al. 2024) and total variation distance (Chen et al. 2022, Lee et al. 2023). The upper bound of $\epsilon_{\text{distribution}}$ generally takes the form,

$$\epsilon_{\text{distribution}} \lesssim \epsilon_{\text{score}} + \text{discretization-error} + \text{forward-error}, \quad (3.1)$$

where ϵ_{score} is the score estimation error in L_2 or L_∞ , discretization-error accounts for errors from discretizing the SDE, and forward-error quantifies the distance between \mathbf{X}_T and the reference standard Gaussian distribution, which decays exponentially with respect to T . Chen et al. (2022) and Lee et al. (2023) studied $\epsilon_{\text{distribution}}$ in terms of total variation distances, assuming L_2 accurate score estimation, in contrast to L_∞ accurate score estimation assumption in De Bortoli et al. (2021). These analyses were conducted under regularity conditions on the target distribution. The number of discretization required in Chen et al. (2022) and Lee et al. (2023) scales polynomially with the dimension of the target distribution. Benton et al. (2024) provide convergence bounds in terms of KL divergence, which scales linearly with the target distribution dimension up to logarithmic factors, assuming

only finite second moments of the data distribution. These works treat score estimation as a black box and retain ϵ_{score} as a separate term throughout the analysis.

For ϵ_{score} , [Chen, Huang, Zhao & Wang \(2023\)](#) studied a specific neural network construction and demonstrated that the upper bound of sample complexity of score estimation is exponential in the score network dimension. To the best of our knowledge, this is the only theoretical result on the sample complexity of score estimation error, highlighting the curse of ambient dimensionality in data. By constructing the diffusion model in a low-dimensional continuous space, we avoid training a high-dimensional score network, thereby significantly reducing the sample complexity.

4 Simulation studies

In this section, we conduct simulation studies to evaluate the performance of DDE and compare it with its competitors. Note that one can encode a hyperlink as a binary vector valued in $\{0, 1\}^n$, with 1 indicating a node on this hyperlink and 0 otherwise. We study two competitors. This first one is Ber-Diff, which stands for Bernoulli diffusion models for binary-valued vectors ([Sohl-Dickstein et al. 2015](#)). The second one is Gau-Diff, which stands for Gaussian diffusion models on the binary-valued vectors and thresholding for binary outputs using calibration. Detailed descriptions of the algorithms are in the Supplementary Material.

We consider the following simulation setups with embeddings generated in Euclidean spaces. When the latent space dimension is K , the hyperlink embeddings are generated from a K -component Gaussian mixture distribution, where the k th Gaussian distribution follows $\mathcal{N}_{[-2/\sqrt{K}, 0]}(\mathbf{1}_K/(K\sqrt{K}) - \mathbf{e}_k/\sqrt{K}, \mathbf{I})$ for $k = 1, \dots, K$. Here, $\mathbf{1}_K$ is a K -dimensional vector with all 1's, $\mathbf{e}_k \in \{0, 1\}^K$ is a column vector with the k th element being 1 while the other entries being 0. The node embeddings are generated from a K -component Gaussian

mixture with the k th Gaussian follows $\mathcal{N}_{[0,2/\sqrt{K}]}(\mathbf{1}_K/\sqrt{K} + \mathbf{e}_k/\sqrt{K}, \mathbf{I})$. The vertex degree heterogeneity parameters $\{\alpha_i\} \subset \mathbb{R}$ are specified in each setup. After generating m hyperlink embeddings and n node embeddings, we generate a hypergraph $\mathcal{H}([n], \mathcal{E}_m)$ following Example 2.1. Different generative models are then trained on $\mathcal{H}([n], \mathcal{E}_m)$ and generate $32*m$ new hyperlinks. We use the Root Mean Squared Error (RMSE) of means (normalized frequencies) and variance-covariances of node co-occurrence to assess the generative performance of different methods.

First, we consider a small scale setting with $K = 2$ and $m, n \in \{300, 500\}$. We separate this setup with other setup due to the heavy computation burden of Ber-Diff. For different methods, we set the training epochs and batch size to be the same. As Table 1 shows, given the same amount of training epochs, Ber-Diff performs significantly worse than the other two methods, even with a much higher demand for computing resources and running time. DDE and Gau-Diff are comparable, with similar performance on the means and better on the variance-covariances.

m	Method	$n = 300$	$n = 500$
Embedding Dimension $K = 2$			
300	DDE	0.0181	0.0189
	Gau-Diff	0.0177	0.0183
	Ber-Diff	0.1126	0.1159
500	DDE	0.0152	0.0141
	Gau-Diff	0.0147	0.0137
	Ber-Diff	0.0522	0.1127

m	Method	$n = 300$	$n = 500$
Embedding Dimension $K = 2$			
300	DDE	0.0041	0.0039
	Gau-Diff	0.0093	0.0100
	Ber-Diff	0.0382	0.0412
500	DDE	0.0032	0.0031
	Gau-Diff	0.0088	0.0101
	Ber-Diff	0.0124	0.0098

Table 1: RMSE of means (left) and covariances (right) of DDE, Gau-Diff and Ber-Diff. Each value comes from the median of 20 repetitions.

We further scale up the size of the observed hypergraphs. Due to computation resource and time limitation, and due to the significantly worse performance of Ber-Diff, we ignore Ber-Diff and only compare DDE with Gau-Diff. We let $K \in \{2, 4, 8\}$ and $m, n \in \{200, 400, 800, 1600\}$. We consider two sparsity cases with $\{\alpha_i\}$ being i.i.d. sampled from Uniform $[-1, 0]$ in Table 2 and from Uniform $[-2, -1]$ in Table 3. From Table 2,

m	Method	$n = 200$	$n = 400$	$n = 800$	$n = 1600$	m	Method	$n = 200$	$n = 400$	$n = 800$	$n = 1600$
Embedding Dimension $K = 2$						Embedding Dimension $K = 2$					
200	DDE	0.0222	0.0232	0.0227	0.0229	200	DDE	0.0052	0.0049	0.0047	0.0046
	Gau-Diff	0.0220	0.0223	0.0222	0.0222		Gau-Diff	0.0098	0.0099	0.0099	0.0071
400	DDE	0.0170	0.0165	0.0163	0.0163	400	DDE	0.0038	0.0034	0.0033	0.0033
	Gau-Diff	0.0163	0.0159	0.0158	0.0157		Gau-Diff	0.0080	0.0097	0.0102	0.0069
800	DDE	0.0113	0.0117	0.0114	0.0115	800	DDE	0.0028	0.0025	0.0023	0.0023
	Gau-Diff	0.0108	0.0109	0.0111	0.0111		Gau-Diff	0.0066	0.0092	0.0104	0.0070
1600	DDE	0.0087	0.0086	0.0085	0.0085	1600	DDE	0.0022	0.0017	0.0017	0.0016
	Gau-Diff	0.0080	0.0079	0.0078	0.0079		Gau-Diff	0.0057	0.0089	0.0105	0.0073
Embedding Dimension $K = 4$						Embedding Dimension $K = 4$					
200	DDE	0.0240	0.0232	0.0226	0.0229	200	DDE	0.0057	0.0048	0.0044	0.0041
	Gau-Diff	0.0230	0.0227	0.0223	0.0227		Gau-Diff	0.0081	0.0069	0.0059	0.0037
400	DDE	0.0162	0.0166	0.0166	0.0166	400	DDE	0.0040	0.0034	0.0030	0.0028
	Gau-Diff	0.0155	0.0163	0.0160	0.0160		Gau-Diff	0.0063	0.0066	0.0062	0.0034
800	DDE	0.0118	0.0118	0.0121	0.0125	800	DDE	0.0031	0.0024	0.0021	0.0020
	Gau-Diff	0.0112	0.0110	0.0110	0.0111		Gau-Diff	0.0047	0.0062	0.0060	0.0033
1600	DDE	0.0079	0.0092	0.0099	0.0105	1600	DDE	0.0024	0.0017	0.0015	0.0015
	Gau-Diff	0.0077	0.0079	0.0079	0.0079		Gau-Diff	0.0038	0.0060	0.0061	0.0032
Embedding Dimension $K = 8$						Embedding Dimension $K = 8$					
200	DDE	0.0245	0.0239	0.0245	0.0238	200	DDE	0.0059	0.0049	0.0041	0.0039
	Gau-Diff	0.0226	0.0226	0.0230	0.0226		Gau-Diff	0.0073	0.0055	0.0036	0.0028
400	DDE	0.0172	0.0164	0.0165	0.0170	400	DDE	0.0044	0.0039	0.0033	0.0028
	Gau-Diff	0.0163	0.0160	0.0156	0.0160		Gau-Diff	0.0055	0.0051	0.0037	0.0027
800	DDE	0.0121	0.0117	0.0117	0.0117	800	DDE	0.0034	0.0028	0.0023	0.0020
	Gau-Diff	0.0116	0.0115	0.0114	0.0112		Gau-Diff	0.0040	0.0047	0.0032	0.0027
1600	DDE	0.0088	0.0081	0.0084	0.0082	1600	DDE	0.0027	0.0021	0.0017	0.0014
	Gau-Diff	0.0083	0.0079	0.0081	0.0079		Gau-Diff	0.0029	0.0044	0.0023	0.0030

Table 2: RMSE of means (left) & covariances (right) of DDE and Gau-Diff when $\alpha_i \in [-1, 0]$. Each value comes from the median of 20 repetitions.

we can observe that as m increases, the RMSE of means and covariances decreases. DDE has slightly higher RMSEs of means than Gau-Diff. This is reasonable as Gau-Diff is calibrated with the means of the observed data. In terms of RMSE of covariances, DDE has a significantly better performance than Gau-Diff. Last, we consider hypergraphs with higher sparsity in Figure 3, with $\{\alpha_i^*\}$ sampled i.i.d. from Uniform $[-2, -1]$. Table 3 shows that DDE still outperforms Gau-Diff, with similar RMSE of means and significantly lower RMSE of covariances. The result highlights the superiority of DDE when it comes to sparse hypergraphs. More results from simulation studies are provided in the Supplementary Material.

m	Method	$n = 200$	$n = 400$	$n = 800$	$n = 1600$	m	Method	$n = 200$	$n = 400$	$n = 800$	$n = 1600$
Embedding Dimension $K = 2$						Embedding Dimension $K = 2$					
200	DDE	0.0193	0.0186	0.0189	0.0189	200	DDE	0.0035	0.0031	0.0030	0.0029
	Gau-Diff	0.0188	0.0186	0.0184	0.0183		Gau-Diff	0.0051	0.0053	0.0054	0.0053
400	DDE	0.0132	0.0133	0.0133	0.0133	400	DDE	0.0024	0.0022	0.0021	0.0021
	Gau-Diff	0.0128	0.0130	0.0130	0.0130		Gau-Diff	0.0040	0.0052	0.0054	0.0053
800	DDE	0.0093	0.0094	0.0093	0.0090	800	DDE	0.0018	0.0016	0.0015	0.0014
	Gau-Diff	0.0092	0.0091	0.0090	0.0091		Gau-Diff	0.0032	0.0049	0.0053	0.0053
1600	DDE	0.0068	0.0066	0.0068	0.0068	1600	DDE	0.0013	0.0011	0.0010	0.0010
	Gau-Diff	0.0067	0.0063	0.0064	0.0064		Gau-Diff	0.0028	0.0048	0.0053	0.0053
Embedding Dimension $K = 4$						Embedding Dimension $K = 4$					
200	DDE	0.0187	0.0190	0.0189	0.0191	200	DDE	0.0038	0.0033	0.0028	0.0025
	Gau-Diff	0.0182	0.0185	0.0183	0.0186		Gau-Diff	0.0043	0.0037	0.0032	0.0031
400	DDE	0.0138	0.0134	0.0133	0.0133	400	DDE	0.0028	0.0022	0.0019	0.0018
	Gau-Diff	0.0128	0.0132	0.0131	0.0131		Gau-Diff	0.0031	0.0035	0.0032	0.0031
800	DDE	0.0095	0.0095	0.0095	0.0098	800	DDE	0.0021	0.0016	0.0013	0.0012
	Gau-Diff	0.0091	0.0092	0.0093	0.0091		Gau-Diff	0.0023	0.0033	0.0031	0.0030
1600	DDE	0.0070	0.0068	0.0073	0.0075	1600	DDE	0.0016	0.0011	0.0009	0.0009
	Gau-Diff	0.0065	0.0064	0.0065	0.0065		Gau-Diff	0.0018	0.0031	0.0031	0.0030
Embedding Dimension $K = 8$						Embedding Dimension $K = 8$					
200	DDE	0.0196	0.0193	0.0196	0.0196	200	DDE	0.0043	0.0035	0.0028	0.0023
	Gau-Diff	0.0191	0.0182	0.0186	0.0182		Gau-Diff	0.0039	0.0030	0.0022	0.0020
400	DDE	0.0140	0.0134	0.0134	0.0136	400	DDE	0.0031	0.0026	0.0021	0.0017
	Gau-Diff	0.0135	0.0131	0.0129	0.0130		Gau-Diff	0.0028	0.0028	0.0020	0.0018
800	DDE	0.0100	0.0098	0.0094	0.0094	800	DDE	0.0023	0.0019	0.0015	0.0013
	Gau-Diff	0.0095	0.0091	0.0091	0.0090		Gau-Diff	0.0020	0.0026	0.0020	0.0018
1600	DDE	0.0070	0.0069	0.0067	0.0067	1600	DDE	0.0017	0.0013	0.0011	0.0009
	Gau-Diff	0.0067	0.0067	0.0064	0.0065		Gau-Diff	0.0015	0.0025	0.0019	0.0018

Table 3: RMSE of means (left) & covariances (right) of DDE and Gau-Diff when $\alpha_i \in [-2, -1]$. Each value comes from the median of 20 repetitions.

5 The symptom co-occurrence hypergraph

In this section, we apply DDE and other competitive approaches to a symptom co-occurrence hypergraph constructed from electronic medical records. We use the Medical Information Mart for Intensive Care (MIMIC-III; [Johnson et al. 2016](#)) dataset, which contains clinical data from over 45,000 patients admitted to the ICU of the Beth Israel Deaconess Medical Center in Boston, between the years of 2001 and 2012. We focus on the top 1,000 symptoms by the frequency of their appearance, and construct the hypergraph based on co-occurrence of these symptoms in patient profiles in MIMIC-III. Specifically, each node in this hypergraph represents a symptom, and each hyperlink is constructed based on a

patient profile, with the nodes on it being the symptoms marked on the corresponding patient profile upon discharge from the unit. This results in 41,974 hyperlinks with orders greater than 2. The node degree heterogeneity and hyperlink sparsity are summarized in Figure 3. Among the 41,974 patient profiles, all profiles were marked with fewer than 100 symptoms, with the majority marked around 10, which is significantly smaller than the total of 1,000 symptoms considered. Among the 1,000 nodes, their frequency of appearances ranges from 38 to 17,595, with Code 401.9 (“unspecified essential hypertension”) appearing 17,595 times as the most frequent and Code 767.19 (“other injuries to scalp”) appearing 38 times as the least frequent.

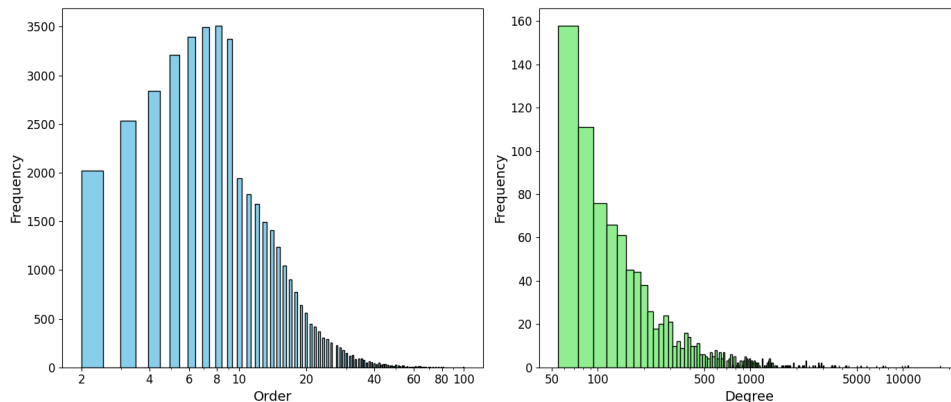


Figure 3: Orders of hyperlinks (left) & degrees of nodes (right) in the symptom co-occurrence hypergraph. The hypergraph has 1,000 nodes and 41,974 hyperlinks.

We train generative models using the observed hypergraph. Due to limitations in computing resources and device memory, only DDE can be trained on the entire dataset of 41,974 hyperlinks. To ensure a fair comparison among the approaches, we reduce the number of hyperlinks and focus on the top m hyperlinks with the highest orders, where $m \in \{1000, 2000, 3000\}$. We use each approach to generate $32 * m$ hyperlinks. The performance of each approach is evaluated based on the RMSE of the sample means and sample covariances of the generated hyperlinks, compared to the sample means and sample covariances of the total 41,974 hyperlinks. As shown in Table 4, DDE outperforms the other

methods, achieving the lowest errors in the first and second moments of the generated hyperlinks. The performance remains consistent across various choices of the latent space dimension K . Meanwhile, DDE also requires the least computational resources and time. The training and sampling time of Gau-Diff is 1.2-1.5 times that of DDE using the same computing resources, and Ber-Diff is 100-500 slower than DDE, even with more powerful computing resources. Ber-Diff also has the highest memory usage, as it encounters out-of-memory(OOM) errors when training with sample sizes larger than or equal to 2,000. This analysis demonstrates that DDE can efficiently and accurately generate new hyperlinks that preserve key statistical information about symptom co-occurrences in medical records (e.g., means and covariances), without privacy leakage. Consequently, a medical institution planning to release patient symptom data for research purposes could apply DDE to the dataset prior to its release.

Method	$m = 1000$	$m = 2000$	$m = 3000$
DDE (K=2)	0.0713	0.0574	0.0505
DDE (K=4)	0.0717	0.0585	0.0515
DDE (K=8)	0.0714	0.0565	0.0516
Gau-Diff	0.2109	0.2702	0.2108
Ber-Diff	0.4108	OOM	OOM

Method	$m = 1000$	$m = 2000$	$m = 3000$
DDE (K=2)	0.0024	0.0019	0.0017
DDE (K=4)	0.0025	0.0021	0.0018
DDE (K=8)	0.0026	0.0021	0.0019
Gau-Diff	0.0041	0.0049	0.0040
Ber-Diff	0.0524	OOM	OOM

Table 4: RMSE of means (left) & covariances (right) for DDE, Gau-Diff, and Ber-Diff. OOM stand for “out of memory”.

6 Discussion

This paper introduces a generative model architecture, Denoising Diffused Embeddings (DDE), for hypergraphs. Based on a likelihood model for hyperlinks, this approach first embeds the hyperlinks and nodes in the hypergraph in a latent space. The new hyperlink embeddings are then sampled from diffusion models trained on the estimated hyperlink

embeddings. Following the likelihood model, new hyperlinks are subsequently generated based on the sampled new hyperlink embeddings and the estimated node embeddings and degrees. In contrast to many generative models designed for continuous data, DDE naturally handles the discreteness of hyperlinks. Furthermore, the likelihood modeling in DDE offers interpretability and captures unique properties of hypergraphs such as node degree heterogeneity and hyperlink sparsity. The use of diffusion models also enables DDE for the private generation of new hyperlinks, which has important applications in areas such as electronic health record analysis.

Theoretically, we analyze the generative performance of DDE. Under ideal conditions where embeddings are available, DDE effectively reduces the problem of generating high-dimensional hyperlinks to generating low-dimensional embeddings. When the estimation of embeddings is incorporated into the process, we examine how factors such as dimensionality, node degree heterogeneity, and hyperlink sparsity affect the generative performance. These analyses are not only of theoretical interest, but also provide practical guidance on when to apply DDE for hypergraph generation tasks.

Future work could focus on the effective design of score neural networks to better accommodate hypergraph model structures. Although the current DDE architecture is applicable to any hypergraph model, tailoring the score network to specific hypergraph models has the potential to circumvent the estimation of hyperlink embeddings, such as the work in [Chen, Huang, Zhao & Wang \(2023\)](#) for data residing in a linear subspace. This could improve the performance of the generative model, particularly in scenarios where m (the number of hyperlinks) is significantly larger than n (the number of nodes). The selection of hypergraph models within this framework is also of great interest, either through prior knowledge of the hypergraph generation process or via a data-adaptive approach. Furthermore, analyzing and justifying the privacy of the generated hyperlinks could further highlight the contributions of such generative model architectures.

References

- Austin, J., Johnson, D. D., Ho, J., Tarlow, D. & Van Den Berg, R. (2021), ‘Structured denoising diffusion models in discrete state-spaces’, *Advances in Neural Information Processing Systems* **34**, 17981–17993.
- Bai, J. & Li, k. (2012), ‘Statistical analysis of factor models of high dimension’, *The Annals of Statistics* **40**(1), 436–465.
- Benton, J., Bortoli, V., Doucet, A. & Deligiannidis, G. (2024), ‘Nearly d-linear convergence bounds for diffusion models via stochastic localization’.
- Chen, M., Huang, K., Zhao, T. & Wang, M. (2023), ‘Score approximation, estimation and distribution recovery of diffusion models on low-dimensional data’, pp. 4672–4712.
- Chen, M., Mei, S., Fan, J. & Wang, M. (2024), ‘Opportunities and challenges of diffusion models for generative AI’, *National Science Review* p. nwae348.
- Chen, S., Chewi, S., Li, J., Li, Y., Salim, A. & Zhang, A. R. (2022), ‘Sampling is as easy as learning the score: theory for diffusion models with minimal data assumptions’, *arXiv preprint arXiv:2209.11215*.
- Chen, X., He, J., Han, X. & Liu, L. (2023), Efficient and degree-guided graph generation via discrete diffusion modeling, *in* ‘International Conference on Machine Learning’, PMLR, pp. 4585–4610.
- Creswell, A., White, T., Dumoulin, V., Arulkumaran, K., Sengupta, B. & Bharath, A. A. (2018), ‘Generative adversarial networks: An overview’, *IEEE signal processing magazine* **35**(1), 53–65.
- De Bortoli, V., Thornton, J., Heng, J. & Doucet, A. (2021), ‘Diffusion schrödinger bridge with applications to score-based generative modeling’, *Advances in Neural Information Processing Systems* **34**, 17695–17709.
- Ghoshdastidar, D. & Dukkipati, A. (2015), A provable generalized tensor spectral method for uniform hypergraph partitioning, *in* ‘International Conference on Machine Learning’, PMLR, pp. 400–409.
- Ghoshdastidar, D. & Dukkipati, A. (2017), ‘Consistency of spectral hypergraph partitioning under planted partition model’, *The Annals of Statistics* **45**, 289–315.
- Goodfellow, I., Pouget-Abadie, J., Mirza, M., Xu, B., Warde-Farley, D., Ozair, S., Courville, A. & Bengio, Y. (2020), ‘Generative adversarial networks’, *Communications of the ACM* **63**(11), 139–144.
- Ho, J., Jain, A. & Abbeel, P. (2020), ‘Denoising diffusion probabilistic models’, *Advances in neural information processing systems* **33**, 6840–6851.
- Huang, C.-W., Aghajohari, M., Bose, J., Panangaden, P. & Courville, A. C. (2022), ‘Riemannian diffusion models’, *Advances in Neural Information Processing Systems* **35**, 2750–2761.
- Johnson, A. E., Pollard, T. J., Shen, L., Lehman, L.-w. H., Feng, M., Ghassemi, M., Moody, B., Szolovits, P., Anthony Celi, L. & Mark, R. G. (2016), ‘MIMIC-III, a freely accessible critical care database’, *Scientific Data* **3**(1), 1–9.

- Ke, Z. T., Shi, F. & Xia, D. (2019), ‘Community detection for hypergraph networks via regularized tensor power iteration’, *arXiv preprint arXiv:1909.06503* .
- Kingma, D. P. (2013), ‘Auto-encoding variational bayes’, *arXiv preprint arXiv:1312.6114* .
- Kingma, D. P., Welling, M. et al. (2019), ‘An introduction to variational autoencoders’, *Foundations and Trends® in Machine Learning* **12**(4), 307–392.
- Kumar, T., Vaidyanathan, S., Ananthapadmanabhan, H. & Parthasarathy, S. (2018), ‘Hypergraph clustering: A modularity maximization approach. arxiv 2018’, *arXiv preprint arXiv:1812.10869* .
- Lee, H., Lu, J. & Tan, Y. (2023), Convergence of score-based generative modeling for general data distributions, *in* ‘International Conference on Algorithmic Learning Theory’, PMLR, pp. 946–985.
- Lee, J., Kim, D. & Chung, H. W. (2020), ‘Robust hypergraph clustering via convex relaxation of truncated mle’, *IEEE Journal on Selected Areas in Information Theory* **1**(3), 613–631.
- Li, J., Xu, G. & Zhu, J. (2023), ‘Statistical inference on latent space models for network data’, *arXiv preprint arXiv:2312.06605* .
- Li, S. & Schramm, T. (2023), ‘Spectral clustering in the gaussian mixture block model’, *arXiv preprint arXiv:2305.00979* .
- Lou, A., Meng, C. & Ermon, S. (2024), Discrete diffusion modeling by estimating the ratios of the data distribution, *in* ‘Forty-first International Conference on Machine Learning’.
- Lu, C., Zhou, Y., Bao, F., Chen, J., Li, C. & Zhu, J. (2022), ‘Dpm-solver: A fast ode solver for diffusion probabilistic model sampling in around 10 steps’, *Advances in Neural Information Processing Systems* **35**, 5775–5787.
- Nepusz, T., Yu, H. & Paccanaro, A. (2012), ‘Detecting overlapping protein complexes in protein-protein interaction networks’, *Nature methods* **9**(5), 471–472.
- Rhodes, D. R., Tomlins, S. A., Varambally, S., Mahavisno, V., Barrette, T., Kalyanasundaram, S., Ghosh, D., Pandey, A. & Chinnaiyan, A. M. (2005), ‘Probabilistic model of the human protein-protein interaction network’, *Nature biotechnology* **23**(8), 951–959.
- Rinaldo, A., Bacanu, S.-A., Devlin, B., Sonpar, V., Wasserman, L. & Roeder, K. (2005), ‘Characterization of multilocus linkage disequilibrium’, *Genetic epidemiology* **28**(3), 193–206.
- Rombach, R., Blattmann, A., Lorenz, D., Esser, P. & Ommer, B. (2022), High-resolution image synthesis with latent diffusion models, *in* ‘Proceedings of the IEEE/CVF conference on computer vision and pattern recognition’, pp. 10684–10695.
- Shojaie, A. & Michailidis, G. (2009), ‘Analysis of gene sets based on the underlying regulatory network’, *Journal of Computational Biology* **16**(3), 407–426.
- Sohl-Dickstein, J., Weiss, E., Maheswaranathan, N. & Ganguli, S. (2015), Deep unsupervised learning using nonequilibrium thermodynamics, *in* ‘International conference on machine learning’, PMLR, pp. 2256–2265.

- Song, Y., Dhariwal, P., Chen, M. & Sutskever, I. (2023), ‘Consistency models’, *arXiv preprint arXiv:2303.01469* .
- Song, Y., Sohl-Dickstein, J., Kingma, D. P., Kumar, A., Ermon, S. & Poole, B. (2020), ‘Score-based generative modeling through stochastic differential equations’, *arXiv preprint arXiv:2011.13456* .
- Thibeault, V., Allard, A. & Desrosiers, P. (2024), ‘The low-rank hypothesis of complex systems’, *Nature Physics* **20**(2), 294–302.
- Vahdat, A., Kreis, K. & Kautz, J. (2021), ‘Score-based generative modeling in latent space’, *Advances in neural information processing systems* **34**, 11287–11302.
- Wang, F. (2022), ‘Maximum likelihood estimation and inference for high dimensional generalized factor models with application to factor-augmented regressions’, *Journal of Econometrics* **229**(1), 180–200.
- Wu, S., Xu, G. & Zhu, J. (2024), ‘A general latent embedding approach for modeling non-uniform high-dimensional sparse hypergraphs with multiplicity’, *arXiv preprint arXiv:2410.12108* .
- You, J., Ying, R., Ren, X., Hamilton, W. & Leskovec, J. (2018), Graphrnn: Generating realistic graphs with deep auto-regressive models, *in* ‘International conference on machine learning’, PMLR, pp. 5708–5717.
- Yuan, M., Liu, R., Feng, Y. & Shang, Z. (2022), ‘Testing community structure for hypergraphs’, *The Annals of Statistics* **50**(1), 147–169.
- Yuan, Y. & Qu, A. (2023), ‘High-order joint embedding for multi-level link prediction’, *Journal of the American Statistical Association* **118**(543), 1692–1706.
- Zhen, Y. & Wang, J. (2023), ‘Community detection in general hypergraph via graph embedding’, *Journal of the American Statistical Association* **118**(543), 1620–1629.